Electronic Supplementary Material (ESI) for Journal of Materials Chemistry C.
This journal is © The Royal Society of Chemistry 2017

Supporting Information for:

Effects of *meso*-M(PPh_3)$_2$Cl (M = Pd, Ni) substituents on the linear and third-order nonlinear optical properties of chalcogenopyrylium-terminated heptamethines in solution and solid states

Iryna Davydenko,[a] Sepehr Benis,[b] Stephen B. Shiring,[a] Janos Simon,[a] Rajesh Sharma,[b,c] Taylor G. Allen,[a] San-Hui Chi,[a] Qing Zhang,[a] Yulia A. Getmanenko,[a] Timothy C. Parker,[a] Joseph W. Perry,[a] Jean-Luc Brédas,[a] David J. Hagan,[b] Eric W. Van Stryland,[b] Stephen Barlow,[a] Seth R. Marder[a]*

[a]*School of Chemistry and Biochemistry and Center for Organic Photonics and Electronics, Georgia Institute of Technology, Atlanta, Georgia 30332-0400, United States*

[b]*CREOL, The College of Optics and Photonics, University of Central Florida, Orlando, Florida 32816, United States*

[c]*Department of Physics, University Institute of Sciences, Chandigarh University, Mohali, Punjab 140413, India*

CONTENTS:

1. Experimental Details for Synthesis and Molecular Characterisation

1.1. General Details

All reagents were purchased from commercial sources and were used without further purification, or were synthesised according to cited literature. ^{1}H, ^{13}C, and ^{31}P NMR spectra were recorded by using a Varian 300, Bruker 400, or Bruker Avance IIIHD 500 instrument. Chemical shifts are listed in parts per million (ppm) and were referenced using the residual solvent ^{1}H signal or the solvent ^{13}C resonance; the ^{31}P NMR data were referenced externally to H_3PO_4 (δ = 0 ppm). Column chromatography was carried out using silica gel (60 Å, 40-63 μm, Sorbent) as the stationary phase. Mass spectra were measured on an Applied Biosystems 4700 Proteomics Analyzer using MALDI or a VG Instruments 70-SE using electron impact (EI) mode. Molar absorptivities (ε) in chloroform (spectrophotometric grade) solution (ca. 10^{-5} M) were determined at least twice for each compound in a 1 cm quartz cuvette using a Varian Cary 5E spectrometer. Thermogravimetric analysis (TGA) analyses were recorded using a NETZSCH STA 449C. Cyclic voltammetry (CV) was carried out under an inert atmosphere in dry deoxygenated dichloromethane solution containing 0.1 M tetrabutylammonium hexafluorophosphate as electrolyte, a CH Instrument 620D potentiostat, a glassy carbon working electrode, platinum wire counter electrode, and a silver wire coated with silver chloride as the pseudo-reference electrode. Cyclic voltammograms were recorded at a scan rate of 50 mV s^{-1}. Elemental analyses were carried out by Atlantic Microlabs using a LECO 932 CHNS elemental analyzer.

1.2. Synthesis of *meso*-M(PPh$_3$)$_2$Cl-Substituted Dyes

The palladium- and nickel-substituted dyes, **1Pd-5Pd**, **1'Pd**, and **1Ni** were synthesised from the corresponding chloro dyes, **1Cl-5Cl**, **1'Cl** as shown in Scheme 1. The preparation of the chloro dyes is described in section 1.3.

General Procedure for M(PPh$_3$)$_2$Cl-Substituted Dyes. The appropriate *meso*-chloro dye was dissolved in a solvent, and deoxygenated. M(PPh$_3$)$_4$ (1 eq.) was added and the reaction mixture was stirred at room temperature (unless otherwise stated) under nitrogen. The solvent was removed under vacuum and the residue was washed with hexane (for **4Pd** and **5Pd**), and purified by column chromatography on silica gel, followed by (except for **4Pd** and **5Pd**) extraction into CH_2Cl_2, filtration, and evaporation.

1'Pd. From **1'Cl** (0.075 g, 0.1 mmol) and Pd(PPh$_3$)$_4$ (0.116 g, 0.1 mmol) in $CHCl_3$ / MeCN (1:2; 30 mL) for 12 h. Eluent: $CHCl_3$ / MeOH (99:1 changing to 97:3). Yield: 0.087 g, 63%. ^{1}H NMR (500 MHz, (CD_2Cl_2): δ 9.00 (d, $^{3}J_{HH}$ = 13.8 Hz, 2H), 7.84–7.40 (m, 36H), 7.30 (t, $^{3}J_{HH}$ = 7.5 Hz, 6H), 7.11 (t, $^{3}J_{HH}$ = 7.7 Hz, 12H), 6.31 (d, $^{3}J_{HH}$ = 13.8 Hz, 2H), 1.73 (t, $^{3}J_{HH}$ = 5.8 Hz, 4H), 0.76 (quin., $^{3}J_{HH}$ = 6.0 Hz, 2H). ^{13}C{^{1}H} NMR (125 MHz, (CD_2Cl_2): δ 206.55, 149.70, 149.00 (br. s), 147.39, 146.03, 136.10, 134.27

(app.t, J_{CP} = 6.0 Hz), 131.23, 130.66 (app.t, J_{CP} = 23 Hz), 130.60, 129.71, 128.11(app. t, J_{CP} = 6.0 Hz), 126.80, 122.53, 121.00 (br. s), 27.36, 20.04. ^{31}P NMR (202.5 MHz, (CD_2Cl_2): δ 21.55 (s). HRMS (ESI+): *m/z* 1291.2658 (calculated for $C_{80}H_{64}ClP_2PdS_2$ 1291.2643, ($[M–BF_4]^+$)). Anal. calcd. for $C_{80}H_{64}BClF_4P_2PdS_2$: C, 69.62; H, 4.67; S, 4.65. Found: C, 70.03; H, 5.02; S, 4.37.

1Pd. From **1Cl** (0.081 g, 0.053 mmol) and $Pd(PPh_3)_4$ (0.061 g, 0.053 mmol) in $CHCl_3$ (10 mL) for 2 h. Eluent: hexane / CH_2Cl_2 (2:3). Yield: 0.071 g, 62%. ^{1}H NMR (500 MHz, ($CDCl_3$): δ 9.08 (d, $^3J_{HH}$ = 13.8 Hz, 2H), 7.80–7.45 (m, 46H), 7.23 (t, $^3J_{HH}$ = 7.5 Hz, 6H), 7.06 (t, $^3J_{HH}$ = 7.6 Hz, 12H), 6.21 (d, $^3J_{HH}$ = 13.8 Hz, 2H), 1.65 (t, $^3J_{HH}$ = 5.8 Hz, 4H), 0.65 (quin., $^3J_{HH}$ = 6.0 Hz, 2H) (1 peak missing, presumably due to overlap with the residual solvent peak from $CDCl_3$). $^{13}C\{^1H\}$ NMR (125 MHz, ($CDCl_3$): δ 208.21 (t, J_{CP} = 2.5 Hz), 161.62 (1:1:1:1 q, J_{CB} = 50 Hz), 151.05, 149.54, 148.89, 147.42, 145.76 (t, J_{CP} = 2.3 Hz), 136.08, 135.57, 134.70, 134.21 (app. t, J_{CP} = 6.0 Hz), 131.45, 131.18, 130.62 (app. t, J_{CP} = 23 Hz), 130.52, 129.82, 129.50, 128.78 (qq, J_{CF} = 31, 3Hz), 128.05 (app.t, J_{CP} = 6.0 Hz), 127.03, 126.28, 124.45 (q, J_{CF} = 272 Hz), 121.86, 120.73, 117.33 (sept., J_{CF} = 3.8 Hz), 27.18, 19.75. ^{31}P NMR (202.5 MHz, ($CDCl_3$): δ 21.30 (s). HRMS (MALDI): *m/z* 767.0790 (calculated for $C_{44}H_{34}S_2ClPd$ 767.0792, ($[M–2PPh_3\text{-}BAr'_4]^+$)). Anal. calcd. for $C_{112}H_{76}BClF_{24}P_2PdS_2$: C, 62.38; H, 3.55; S, 2.97. Found: C, 62.54; H, 3.83; S, 2.96.

1Ni. From **1Cl** (0.081 g, 0.053 mmol) and $Ni(PPh_3)_4$ (0.059 g, 0.053 mmol) in $CHCl_3$ (10 mL) for 2 h. Eluent: $CHCl_3$. Yield: 0.073 g, 65%. ^{1}H NMR (500 MHz, ($CDCl_3$): δ 10.01 (d, $^3J_{HH}$ = 13.5 Hz, 2H), 7.84 (s, 2H), 7.75–7.50 (m, 44H), 7.22 (t, $^3J_{HH}$ = 7.5 Hz, 6H), 7.07 (t, $^3J_{HH}$ = 7.5 Hz, 12H), 6.20 (d, $^3J_{HH}$ = 13.5 Hz, 2H), 1.60 (t, $^3J_{HH}$ = 6.5 Hz, 4H), 0.54 (quin., $^3J_{HH}$ = 6.0 Hz, 2H) (1 peak missing, presumably due to overlap with the residual solvent peak from $CDCl_3$). $^{13}C\{^1H\}$ NMR (125 MHz, ($CDCl_3$): δ 161.61 (1:1:1:1 q, J_{CB} = 50 Hz), 149.51, 149.08, 148.15, 147.85, 146.91, 136.12, 135.68, 134.70, 134.18 (app.t, J_{CP} = 5.1 Hz), 131.27, 131.12, 130.71 (app.t, J_{CP} = 22 Hz), 130.26, 129.65, 129.51, 128.78 (qq, J_{CF} = 31, 3Hz), 127.95 (app. t, J_{CP} = 5.0 Hz), 127.03, 126.27, 124.46 (q, J_{CF} = 272 Hz), 121.45, 120.92, 117.32 (sept., J_{CF} = 3.5 Hz), 26.93, 19.77. ^{31}P NMR (202.5 MHz, ($CDCl_3$): δ 17.60 (s). HRMS (MALDI): *m/z* 719.1115 (calculated for $C_{44}H_{34}S_2ClNi$ 719.1144, ($[M–2PPh_3\text{-}BAr'_4]^+$)). Anal. calcd. for $C_{112}H_{76}BClF_{24}NiP_2S_2$: C, 63.79; H, 3.63; S, 3.04. Found: C, 63.93; H, 3.57; S, 2.94.

2Pd. From **2Cl** (0.084 g, 0.053 mmol) and $Pd(PPh_3)_4$ (0.061 g, 0.053 mmol) in $CHCl_3$ (10 mL) for 2 h. Eluent: hexane / CH_2Cl_2 (2:3). Yield: 0.077 g, 66%. ^{1}H NMR (500 MHz, ($CDCl_3$): δ 9.10 (d, $^3J_{HH}$ = 13.8 Hz, 2H), 7.78–7.71 (m, 14H), 7.70–7.61 (m, 21H), 7.55–7.48 (m, 10H), 7.32 (s, 2H), 7.20 (t, $^3J_{HH}$ = 7.5 Hz, 3H), 7.12 (t, $^3J_{HH}$ = 7.6 Hz, 6H), 6.99 (t, $^3J_{HH}$ = 7.7 Hz, 6H), 6.22 (d, $^3J_{HH}$ = 13.8 Hz, 2H), 2.03 (dd, $^2J_{HH}$ = 13.8 Hz, $^3J_{HH}$ = 3.1 Hz, 2H), 0.97 (dd, $^2J_{HH}$ = 13.8, $^3J_{HH}$ = 13.8 Hz, 2H), 0.67 (s, 9H), –0.18 (tt, $^2J_{HH}$

= 12.8 Hz, $^3J_{HH}$ = 3.5 Hz, 1H) (two peaks are missing, presumably due to overlap with the residual solvent peak from $CDCl_3$). $^{13}C\{^1H\}$ NMR (125 MHz, ($CDCl_3$): δ 207.44 (m), 161.61 (1:1:1:1 q, J_{CB} = 50 Hz), 149.96, 149.60, 148.93, 147.41, 146.32, 136.08, 135.54, 134.70, 134.38 (app.t, J_{CP} = 5.8 Hz), 134.12 (app. t, J_{CP} = 5.8 Hz), 131.49, 131.21, 130.96, 130.76, 130.60 (app.t, J_{CP} = 25 Hz), 130.56, 130.47, 129.83, 129.49, 128.76 (qq, J_{CF} = 31, 3Hz), 128.09 (app.t, J_{CP} = 5.8 Hz), 128.05(app.t, J_{CP} = 5.8 Hz), 127.03, 126.30, 124.44 (q, J_{CF} = 272 Hz), 121.61, 120.71, 117.33 (sept., J_{CF} = 3.6 Hz), 40.47, 31.93, 29.59, 28.38, 26.61. ^{31}P NMR (202.5 MHz, $CDCl_3$): δ 21.46 (d, J_{PP} = 417 Hz), 21.12 (d, J_{PP} = 417 Hz). HRMS (MALDI): *m/z* 823.1297 (calculated for $C_{48}H_{42}S_2ClPd$ 823.1451, ($[M–2PPh_3\text{-}BAr'_4]^+$)). Anal. calcd. for $C_{116}H_{84}BClF_{24}P_2PdS_2$: C, 62.97; H, 3.83; S, 2.90. Found: C, 62.86; H, 3.98; S, 3.01.

3Pd. From **3Cl** (0.10 g, 0.053 mmol) and $Pd(PPh_3)_4$ (0.061 g, 0.053 mmol) in $CHCl_3$ (10 mL) for 2 h. Eluent: hexane / CH_2Cl_2 (1:1, changing to 3:7). Yield: 0.082 g, 61%. ^1H NMR (500 MHz, ($CDCl_3$): δ 8.85 (d, $^3J_{HH}$ = 13.8 Hz, 2H), 7.71–7.36 (m, 44H), 7.33 (t, $^3J_{HH}$ = 7.8 Hz, 3H), 7.32 (t, $^3J_{HH}$ = 7.8 Hz, 3H), 7.09 (t, $^3J_{HH}$ = 7.6 Hz, 6H), 7.05 (t, $^3J_{HH}$ = 7.6 Hz, 6H), 6.13 (d, $^3J_{HH}$ = 13.8 Hz, 2H), 1.96 (dd, $^2J_{HH}$ = 13.5 Hz, $^3J_{HH}$ = 3.1 Hz, 2H), 1.25 (s, 18H), 1.17 (s, 18H), 0.88 (dd, $^2J_{HH}$ = 13.5, $^3J_{HH}$ = 13.5 Hz, 2H), 0.62 (s, 9H), –0.18 (tt, $^2J_{HH}$ = 13.5 Hz, $^3J_{HH}$ = 3.1 Hz, 1H). $^{13}C\{^1H\}$ NMR (125 MHz, ($CDCl_3$): δ 205.89, 161.20 (1:1:1:1 q, J_{CB} = 50 Hz), 151.28, 149.03, 148.22, 146.72, 145.78 (t, J_{CP} = 5.8 Hz), 138.22, 136.55, 134.70, 134.44 (dd, J_{CP} = 7.2, 4.8 Hz), 134.22 (dd, J_{CP} = 7.2, 4.8 Hz), 133.05, 131.49, 130.96, 130.82, 130.76, 130.71, 130.59, 130.54, 130.40, 130.14, 128.75 (qq, J_{CF} = 31, 3Hz), 128.01 (overlaping peaks), 124.46 (q, J_{CF} = 272 Hz), 123.76, 122.55, 122.08, 121.49, 117.31 (sept., J_{CF} = 3.7 Hz), 105.62, 104.12, 40.37, 31.87, 30.75, 30.42, 28.55, 28.07, 26.59. ^{31}P NMR (202.5 MHz, $CDCl_3$): δ 22.61 (d, J_{PP} = 417 Hz), 22.02 (d, J_{PP} = 417 Hz). HRMS (MALDI): *m/z* 1143.3903 (calculated for $C_{72}H_{74}S_2ClPd$ ($[M–2PPh_3\text{-}BAr'_4]^+$): 1143.3955). Anal. calcd. for $C_{140}H_{116}BClF_{24}P_2PdS_2$: C, 66.38; H, 4.62; S, 2.53. Found: C, 66.54; H, 4.78; S, 2.51.

4Pd. From **4Cl** (50 mg 0.026 mmol) and $Pd(PPh_3)_4$ (30 mg, 0.026 mmol) in anhydrous toluene (4 mL) for 1 h. Eluent: hexane / CH_2Cl_2 (gradient elution from 100% hexane to 1:1 mixture) (silica gel treated with NEt_3). Yield: 22 mg, 33%. ^1H NMR (400 MHz, $CDCl_3$): δ 8.86 (d, $^3J_{HH}$ = 14.0 Hz, 2H), 7.72 (br s, 8H), 7.62-7.57 (m, 10H), 7.52 (s, 4H), 7.40-7.22 (m, 24H, overlapping with CHCl3) 6.09 (d, $^3J_{HH}$ = 13.6 Hz, 2H), 2.15 (s, 12H) 2.03-1.70 (m, 46H), 1.00 (t, J = 13.6 Hz, 2H), 0.68 (s, 9H), -0.20 (tt, $^2J_{HH}$ = 13.2 Hz, , $^3J_{HH}$ = 3.2 Hz, 1H) $^{13}C\{^1H\}$ NMR (125 MHz, $CDCl_3$): δ 203.2, 161.7 (1:1:1:1 q, J_{CB} = 50 Hz), 149.3, 148.2, 145.0 (t, J_{CP} = 2.7 Hz), 134.8, 134.6 (t, J_{CP} = 6 Hz), 134.4 (t, J_{CP} = 6 Hz), 131. 2, 131.0, 130.76, 130.70, 130.65, 130.50, 130.35, 128.86 (qq, J_{CF} = 31, 3 Hz), 128.17 (t, J_{CF} = 4.6 Hz), 124.57 (q, J_{CF} = 272 Hz), 123.86, 117.42 (sept., J_{CF} = 3.6 Hz), 43.50, 42.15, 41.26, 36.20, 32.08, 29.72, 28.62, 26.86. $^{31}P\{^1H\}$ NMR (162 MHz, $CDCl_3$): δ 19.41 (d, J_{PP} = 422 Hz), 19.16 (d, J_{PP} = 422 Hz). MS (MALDI): *m/z* 1151.3

([M–2PPh$_3$-BAr′$_4$]$^+$). Anal. Calcd for $C_{132}H_{124}BClF_{24}P_2PdSe_2$: C: 62.44; H: 4.92; Found: C: 62.23; H: 4.68.

5Pd. From **5Cl** (80 mg, 0.040 mmol) and Pd(PPh$_3$)$_4$ (46 mg, 0.040 mmol, 1 eq) in anhydrous toluene (4 mL) at 40 °C for 30 min. Eluent: hexane / CH_2Cl_2 (Gradient elution from 100% hexane to 1:1) (silica gel treated with NEt_3). Followed by size exclusion chromatography in dichloromethane. Yield: 13 mg, 12% (assuming pure **5Cl**). ^{1}H NMR: (500 MHz, $CDCl_3$): δ 8.92 (d, $^3J_{HH}$ = 13.5 Hz, 2H), 7.72 (br s, 8H), 7.59-7.55 (m, 10H), 7.52 (s, 4H), 7.38 (t, $^3J_{HH}$ = 7.5 Hz, 3H), 7.33 – 7.25 (m, 15H, overlapping with CHCl3), 7.22 (t, $^3J_{HH}$ = 7.5 Hz, 6H), 6.20 (d, $^3J_{HH}$ = 13.5 Hz, 2H), 2.15 (s, 12H), 2.06 (dd, $^2J_{HH}$ = 14 Hz, $^3J_{HH}$ = 3.0 Hz, 2H), 1.98-1.67 (m, 44H), 1.07 (dd, $^2J_{HH}$ = 14 Hz, $^3J_{HH}$ = 14 Hz, 2H), 0.71 (s, 9H), –0.13 (tt, $^2J_{HH}$ = 12.8 Hz, $^3J_{HH}$ = 3.0 Hz, 1H) ^{13}C{^{1}H} NMR (125 MHz, $CDCl_3$): δ 202.21, 161.74 (1:1:1:1 q, J_{CB} = 50 Hz), 149.95, 148.77, 146.29 (m), 134.80, 134.64 (app. t, J_{CP} = 6 Hz), 134.37 (app. t, J_{CP} = 6 Hz), 131. 13, 130.96, 130.88, 130.77, 130.55, 130.52, 130.31, 128.85 (qq, J_{CF} = 31, 3Hz), 128.37, 128.17 (m), 124.57 (q, J_{CF} = 272 Hz), 122.42, 117.42 (sept., J_{CF} = 3.8 Hz), 45.64, 44.39, 42.05, 36.85, 32.63, 30.02, 29.57, 27.28. ^{31}P NMR (202.5 MHz, $CDCl_3$): δ 18.70 (appears as s). HRMS (MALDI): *m/z* 1251.3048 (calculated for $C_{64}H_{82}ClPdTe_2$ ([M–2PPh$_3$-BAr′$_4$]$^+$): 1251.3264). Anal. Calcd for $C_{132}H_{124}BClF_{24}P_2PdTe_2$: C: 60.14; H: 4.74; Found: C: 60.43; H: 4.68.

1.3. Synthesis of *meso*-Chloro-Substituted Dyes

Compound **1'Cl** is commercially available and **1Cl** was synthesised from **1'Cl** by counterion metathesis as previously described.[1] The other chloro species were synthesised as shown in Scheme S1; experimental details for **4Cl** are given elsewhere.[2] Compound **I**[3] and the chalcogenopyrylium salts **II**[4,5] and **IV**[6] have previously been reported and were synthesised according to the literature. Thiopyrylium salt **III** and telluropyrylium salt **V** are new compounds; their synthesis is described in section 1.4.

Scheme S1. Synthesis of *meso*-Chloro-Substituted Dyes.

n	Z	R	Y
II	S	Ph	BF_4
III	S	Ar"	PF_6
IV	Se	Ad	PF_6
V	Te	Ad	PF_6

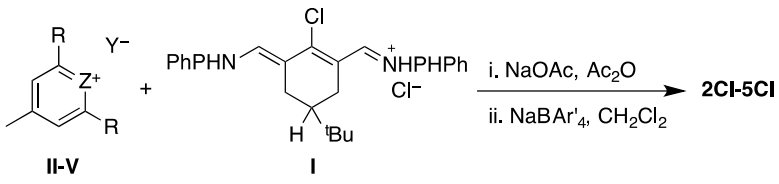

2Cl. A mixture of **II** (0.13 g, 0.37 mmol), **I** (0.079 g, 0.19 mmol), EtOH (3 mL), Ac_2O (0.5 mL), and NaOAc (0.03 g, 0.37 mmol) was heated at 65 ºC (bath temperature) for 45 min under nitrogen. After cooling to room temperature, the precipitate was filtered off and washed with diethyl ether (3 × 2 mL), it was then stirred in CH_2Cl_2 together with NaBAr′$_4$ (0.168 g, 0.19 mmol) for 20 min. The solution was then

evaporated and the residue was purified by column chromatography on silica gel using hexane / CH_2Cl_2 (1:1) as the eluent, followed by dissolution in CH_2Cl_2, filtration, and evaporation. Yield: 0.138 g, 46%. ^{1}H NMR (500 MHz, $CDCl_3$): δ 8.31 (d, $^3J_{HH}$ = 14 Hz, 2H), 7.85 – 7.65 (m, 20H), 7.62 – 7.47 (m, 16H), 6.63 (d, $^3J_{HH}$ = 14 Hz, 2H), 2.97 (dd, $^2J_{HH}$ = 13.5 Hz, $^3J_{HH}$ = 3.0 Hz, 2H), 2.22 (dd, $^2J_{HH}$ = 13.5, $^3J_{HH}$ = 13.5 Hz, 2H), 1.60 (tt, $^2J_{HH}$ = 13.5 Hz, $^3J_{HH}$ = 3.0 Hz, 1H), 1.03 (s, 9H). ^{13}C{^{1}H} NMR (125 MHz, $CDCl_3$): δ 161.60 (1:1:1:1 q, J_{CB} = 50 Hz), 152.68, 149.87, 140.01, 135.44, 134.69, 133.45, 131.71, 129.72, 128.73 (qq, J_{CF} = 32, 3 Hz), 126.73, 125.44 (q, J_{CF} = 273 Hz), 123.11, 121.19, 117.32 (sept., J_{CF} =3.8 Hz), 44.24, 32.30, 28.19, 27.12. HRMS (MALDI): *m/z* 717.2395 (calculated for $C_{48}H_{42}ClS_2$ 717.2411, ([M–BAr′$_4$]$^+$)). Anal. calcd. for $C_{80}H_{54}BClF_{24}S_2$: C, 60.75; H, 3.44. Found: C, 61.04; H, 3.47.

3Cl. A mixture of **III** (0.21 g, 0.37 mmol), **I** (0.079 g, 0.19 mmol), EtOH (3 mL), Ac_2O (0.5 mL), and NaOAc (0.03 g, 0.37 mmol) was heated at 65 ºC (bath temperature) for 45 min under nitrogen. The solvents were removed under reduced pressure and the residue was washed with diethyl ether and filtered. The residue was then stirred in CH_2Cl_2 with NaBAr′$_4$ (0.168 g, 0.19 mmol) for 20 min. The solution was then evaporated and the residue was purified by column chromatography on silica gel using hexane / CH_2Cl_2 (1:1) as the eluent, followed by dissolution in CH_2Cl_2, filtration, and evaporation. Yield: 0.20 g, 58%. ^{1}H NMR (500 MHz, $CDCl_3$): δ 8.28 (d, $^3J_{HH}$ = 14 Hz, 2H), 7.93 (br.s, 4H), 7.72 (br.s, 8H, BAr'$_4$), 7.61 (dd, J = 7.7, 0.8 Hz, 4H), 7.51 (br.s, 4H, BAr'$_4$), 7.49 (dd, J = 7.7, 0.8 Hz, 4H), 7.45 (td, J = 7.5, 1.3 Hz, 4H), 7.40 (td, J = 7.5, 1.3 Hz, 4H), 6.56 (d, $^3J_{HH}$ = 14 Hz, 2H), 2.92 (dd, $^2J_{HH}$ = 13.5 Hz, $^3J_{HH}$ = 2.8 Hz, 2H), 2.19 (dd, $^2J_{HH}$ = 13.5, $^3J_{HH}$ = 13.5 Hz, 2H), 1.56 (m, 1H), 1.23 (s, 36H), 0.99 (s, 9H). ^{13}C{^{1}H} NMR (125 MHz, $CDCl_3$): δ 161.61 (1:1:1:1 q, J_{CB} = 50 Hz), 152.39, 148.48, 148.42, 139.88, 136.68, 134.69, 133.95, 132.70, 130.55, 128.75 (qq, J_{CF} = 32, 3 Hz), 128.58, 128.35, 124.45 (q, J_{CF} = 273 Hz), 122.53, 122.39, 117.31 (sept., J_{CF} =3.8 Hz), 104.74, 42.15, 32.21, 30.65, 28.08 (overlaping peaks), 27.04. HRMS (MALDI): *m/z* 1037.4911(calculated for $C_{72}H_{74}S_2Cl$ 1037.4920, ([M–BAr′$_4$]$^+$)). Anal. calcd. for $C_{104}H_{86}BClF_{24}S_2$: C, 65.67; H, 4.56; S, 3.37. Found: C, 66.58; H, 4.69; S, 3.56.

4Cl. A mixture of **IV** (1.14 g, 2.0 mmol), **I** (0.415 g, 1.0 mmol), Ac_2O (30 mL), and NaOAc (0.172 g, 2.1 mmol) and acetic anhydride (~30 mL) were heated at 65 ºC (bath temperature) for ca. 15 min under nitrogen. The reaction mixture was allowed to cool to room temperature, treated with water, stirred under the flow of nitrogen, and the precipitate was separated by vacuum filtration. Some of the unfiltered mixture was extracted with dichloromethane, the organic phase was combined with the precipitate, and NaBAr′$_4$ (0.94 g, 1.1 mmol) was added. The reaction mixture was stirred for ca. 1 h and purified by column chromatography on silica gel treated with triethylamine, eluting with hexane/ dichloromethane (2:3). The solvents were removed from combined fractions, and product was obtained as dark solid (0.93 g, 48.7% yield). This material was further purified by column chromatography (100 mL of silica gel

treated with ~2 mL of triethylamine, dichloromethane : hexanes (1:1) as eluent). Once the material was loaded onto the column hexanes was used to elute less polar impurity, then dichlomethane : hexanes (1:1) was used to elute the dye. The fractions containing the dye were further purified using a second column on silica gel treated with triethylamine, eluting a yellow-orange impurity first with hexanes and then with hexanes / dichloromethane (1:1) to elute the product (0.78 g, 40.7 % purified yield). ^{1}H NMR (400 MHz, $CDCl_3$): δ 8.30 (d, J = 13.9 Hz, 2H), 7.73 (s, 8H, BAr'$_4$), 7.53 (s, 4H, BAr'$_4$), 7.47 (s, 4H), 6.50 (d, J = 13.9 Hz, 2H), 2.93 (m, 2H), 2.25-2.10 (m, 19H observed), 2.10-1.90 (m, 37H), 1.90-1.60 (m, 46H observed), 1.03 (s, 9H) (74H aliphatic protons are expected, 113H observed, indicating the presence of impurities). DEPT-135 ($CDCl_3$, 100 MHz): δ 139.28 (CH), 134.79 (CH), 124.45 (CH), 117.41 (m, CH), 43.76 (CH_2), 36.14 (CH_2), 28.62 (CH_3), 27.25 (CH) (several minor CH_2 and CH/CH_3 peaks in the aliphatic region provide further evidence for aliphatic impurities). MS (MALDI): *m/z* 1045.2 ([M–BAr'$_4$]$^+$). Anal. Calcd. for $C_{96}H_{94}BClF_{24}Se_2$ C, 60.43; H, 4.97. Found: C, 61.92; H, 5.30. Found: C, 61.94; H, 5.39.

5Cl. A mixture of **V** (328 mg, 0.53 mmol), **I** (100 mg, 0.24 mmol). NaOAc (20 mg, 0.57 mmol), and Ac_2O (5 mL) were heated to 65 ºC for ca. 15 min, after which time it was allowed to cool to room temperature, treated with water, and stirred under a flow of nitrogen; the resulting precipitate was separated by vacuum filtration. The filtrate was also extracted with dichloromethane and these extracts were combined with the precipitate, and stirred with NaBAr′$_4$ (0.21 g) for 1 h, and then evaporated under reduced pressure. The residue was purified by column chromatography on silica gel using hexane / CH_2Cl_2 (1:3) as the eluent. 233 mg, 21%.^{1}H NMR (400 MHz, $CDCl_3$): δ 8.27 (d, J = 13.6 Hz, 2H), 7.73 (s, 8H), 7.53 (s, 4H), 7.47 (s, 4H), 6.45 (d, J = 13.6 Hz, 2H), 2.93 (m, 2H), 2.25-2.10 (m, 12H), 2.10-1.60 (m, 54H), 1.03 (s, 9H). HRMS (MALDI): *m/z* 1145.4213 (calculated for $C_{64}H_{82}Te_2Cl$ 1045.4230, ([M–BAr′$_4$]$^+$)). Satisfactory elemental analysis were not obtained and this compound was converted to **5Pd** without further purification.

1.4. Synthesis of New Precursors to meso-Chloro-Substituted Dyes

Thiopyrylium salt **III** was synthesised as shown in Scheme S2, while telluropyrylium salt **V** was synthesised in an analogous fashion to its Se analogue, **IV**,[6] as shown in Scheme S3.

Scheme S2. Synthesis of Ar"-Substituted Thiopyrylium Salt.

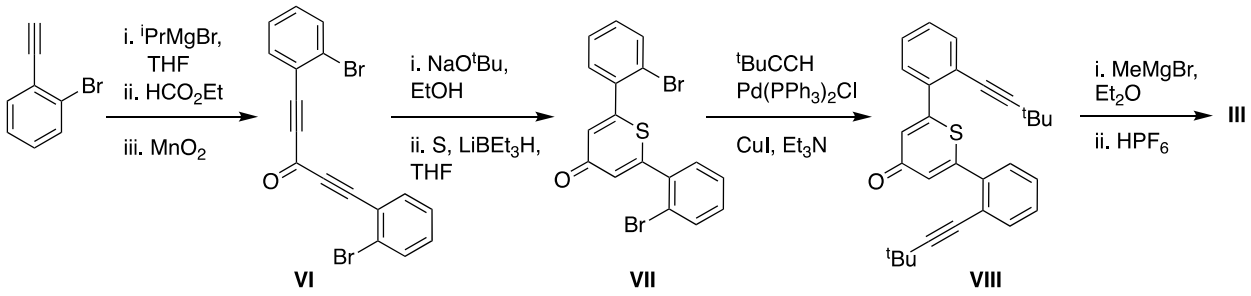

Scheme S3. Synthesis of Ad-Substituted Telluropyrylium Hexafluorophosphate.

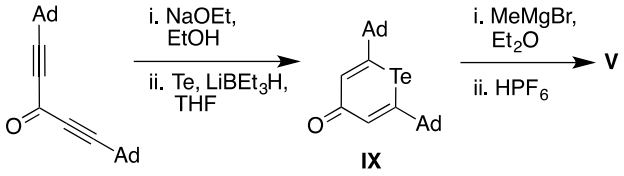

III. MeMgBr (6.68 mL of a 3.0 M solution in THF, 20 mmol) was added to a solution of **VIII** (see below, 1.69 g, 4.0 mmol) in dry deoxygenated THF (25 mL) at 0 °C. After stirring at room temperature for 15 min the solution was poured into AcOH (30 mL). HPF_6 (1.25 mL of a 60% aqueous solution) was added slowly and the mixture was then poured into water (100 mL). THF was removed under reduced pressure and the resulting precipitate was filtered and was washed with water and diethyl ether to yield a yellow solid (1.95 g, 86%). ^{1}H NMR ($CDCl_3$, 300 MHz): δ 8.67 (s, 2H), 7.82-7.76 (m, 2H), 7.66-7.54 (m, 6H), 2.99 (s, 3H), 1.17 (s, 18H). $^{13}C\{^1H\}$ NMR (75 MHz): δ 168.92, 164.57, 136.90, 134.35, 134.02, 132.49, 130.77, 129.54, 122.47, 105.56, 77.24, 30.36, 28.21, 26.24. HRMS-EI: *m/z*: 423.2073 (calculated for $C_{30}H_{31}S$ [$(M\text{-}PF_6)^+$], 423.2146). Anal. Calcd for $C_{30}H_{31}F_6PS$: C, 63.37; H, 5.50; Found: C, 63.55; H, 5.46.

V. MeMgBr (0.94 mL of a 3.0 M solution in Et_2O, 2.84 mmol) was added to a solution of **IX** (see below, 900 mg, 1.89 mmol) in dry deoxygenated THF (20 mL); the mixture was stirred for 1 h and then poured into ice-cold HPF_6 (15 mL of a 65% aqueous solution). The resulting precipitate was filtered, washed with water and diethyl ether and dried in vacuum. ^{1}H NMR (500 MHz, $CDCl_3$): δ 8.26 (s, 2H), 2.78 (s, 3H), 2.52 (bs, 6H), 2.18 (s, 12H), 1.45 (m, 12H) $^{13}C\{^1H\}$ NMR (125 MHz, $CDCl_3$): δ 198.33, 132.40, 45.77, 43.87, 35.68, 28.46. Anal. Calcd for $C_{26}H_{36}F_6PTe$: C, 50.36; H, 5.69; Found: C, 49.52; H, 5.31.

VI. A solution of ^{i}PrMgBr (1.38 mL of a 2.0 M solution in THF, 2.76 mmol) was added slowly to a solution of 1-bromo-2-ethynylbenzene (0.50 g, 2.76 mmol) in THF (5.0 mL) at –78°C under nitrogen. After the addition was complete, the reaction was allowed to warm to 0 °C and HCO_2Et (0.111 mL, 1.38

mmol) was added. The resulting mixture was stirred at room temperature for 30 min. Aqueous NH_4Cl solution was added to the mixture, which was then extracted with diethyl ether (3 × 10 mL). The combined organic layer was dried over $MgSO_4$, filtered, and evaporated under reduced pressure. The residue was purified by column chromatography on silica gel, eluting with hexane / acetone (5:1) to give 1,5-bis(2-bromophenyl)penta-1,4-diyn-3-ol as a colorless and viscous liquid (1.03 g) (^{1}H NMR ($CDCl_3$, 300 MHz): δ 7.57 (dd, J = 7.7, 1.5 Hz, 2H), 7.51 (dd, J = 7.7, 1.5 Hz, 2H), 7.29-7.15 (m, 4H), 5.68 (s, 1H), 2.82 (s, 1H). ^{13}C{^{1}H} NMR (75 MHz, $CDCl_3$): δ 133.75, 132.46, 130.08, 127.03, 125.78, 124.10, 90.09, 83.31, 53.35), which was used in the next step without father purification. The alcohol (14.5 g, 37.12 mmol; a larger portion obtained from a second preparation) was dissolved in CH_2Cl_2 (300 mL) and MnO_2 (25 g, 288 mmol) was added in portions over 24 h with stirring. Once TLC indicated that no starting material remained, the mixture was filtered and solvent was removed under reduced pressure. The residue was purified on silica gel, eluting with hexane / acetone (10:1) to give a white solid (12.5 g, 64% yield for two steps). ^{1}H NMR ($CDCl_3$, 300 MHz): δ 7.70-7.60 (m, 4H), 7.40-7.30 (m, 4H). ^{13}C{^{1}H} NMR (75 MHz, $CDCl_3$): δ 160.32, 135.26, 132.95, 132.32, 127.36, 127.32, 122.06, 92.36, 90.02. HRMS-EI: *m/z* 385.8945 (calculated for $C_{17}H_8Br_2O$ (M^+), 385.8942). Anal. Calcd for $C_{17}H_8Br_2O$: C, 52.62; H, 2.08; Found: C, 52.66; H, 2.05.

VII. NaO^tBu (2.88 g, 30 mmol) was added to **VI** (11.6 g, 30 mmol) in EtOH (40 mL) at room temperature and stirred under nitrogen for 1 h. $LiBEt_3H$ (30 mL of a 1.0 M in THF; 3.0 mmol) was added to sulfur (0.962 g, 30 mmol) in THF (40 mL) and the solution was stirred for 1 h at room temperature. The solution was transferred by cannula to the first and the mixture was stirred at room temperature for 2 h. Water was added to the solution. It was extracted with ether (3 × 200 mL). The combined organic layer was dried over $MgSO_4$, filtered, and evaporated under reduced pressure. The residue was purified by column chromatography on silica gel, eluting with hexane / EtOAc (10:2, changing to 10:3) to give solid **VII** (4.99 g, 40%). ^{1}H NMR ($CDCl_3$, 300 MHz): δ 7.72-7.60 (m, 2H), 7.44-7.40 (m, 4H), 7.35-7.29 (m, 2H), 7.01 (s, 2H). ^{13}C{^{1}H} NMR (75 MHz, $CDCl_3$): δ 181.41, 152.82, 136.36, 133.71, 131.37, 130.82, 130.76, 127.76, 122.27. HRMS-EI: *m/z* 419.8819 (calculated for $C_{17}H_{10}Br_2OS$ (M^+), 419.8819). Anal. Calcd for $C_{17}H_{10}Br_2OS$: C, 48.37; H, 2.39; Found: C, 48.32; H, 2.39.

VIII. 3,3-Dimethylbut-1-yne (2.92 mL, 23.7 mmol) was added to a deoxygenated mixture of **VII** (2.5 g, 5.92 mmol), $PdCl_2(PPh_3)_2$ (83.1 mg, 0.1184 mmol), and CuI (45.1 mg, 0.237 mmol) in NEt_3 (20 mL). The reaction tube was sealed and was heated to 65-70 °C overnight. After cooling to room temperature, the reaction mixture was filtered, and the solvent was removed under reduced pressure. The residue was separated by column chromatography (silica gel) eluting with hexane / EtOAc (10:2 changing to 10:3) to give a slightly green solid (1.75 g, 70%). ^{1}H NMR ($CDCl_3$, 300 MHz): δ 7.54-7.50 (m, 2H), 7.44-7.32 (m,

6H), 7.25 (s, 2H). $^{13}C\{^{1}H\}$ NMR (75 MHz, $CDCl_3$): δ 181.56, 152.72, 137.63, 133.11, 130.14, 129.56, 128.55, 127.80, 122.80, 104.44, 76.89, 30.63, 28.15. HRMS-EI: *m/z* 424.1848 (calculated for $C_{29}H_{28}OS$ (M^+), 424.1861).

IX. $LiBEt_3H$ (5.76 mL of a 1.0 M solution in THF, 5.8 mmol) was added to a deoxygenated suspension of tellurium (368 mg, 2.88 mmol) in anhydrous THF (15 mL). After 1.5 hours stirring, NaOEt (3 mL of a 0.2 M solution in EtOH) was added. Meanwhile, NaOEt (14.4 mL of a 0.2 M solution in EtOH) was added to a solution of 1,5-di(adamantan-1-yl)penta-1,4-diyn-3-one[6] (1.0 g, 2.88 mmol) in anhydrous THF (30 mL) and the mixture was stirred for 30 min; this second solution was then transferred to the reduced tellurium solution, which ws cooled in an ice bath. The combined solution was stirred for 2 h and quenched with aqueous NH_4Cl. The product was extracted with hexanes, dried over $MgSO_4$, and purified using column chromatography. (4:1 CH_2Cl_2 / EtOAc). ^{1}H NMR (500 MHz, $CDCl_3$): δ 7.27 (s, 2H), 2.11 (broad singlet, 6H), 1.91 (s, 12H), 1.73 (m, 12H). $^{13}C\{^{1}H\}$ NMR (125 MHz, $CDCl_3$): δ 208.42, 135.52, 47.99, 45.54, 36.00, 30.21, 28.94. Anal. Calcd for $C_{25}H_{32}OTe$: C, 63.07; H, 6.77; Found: C, 63.25; H, 6.72.

2. Additional Absorption Data

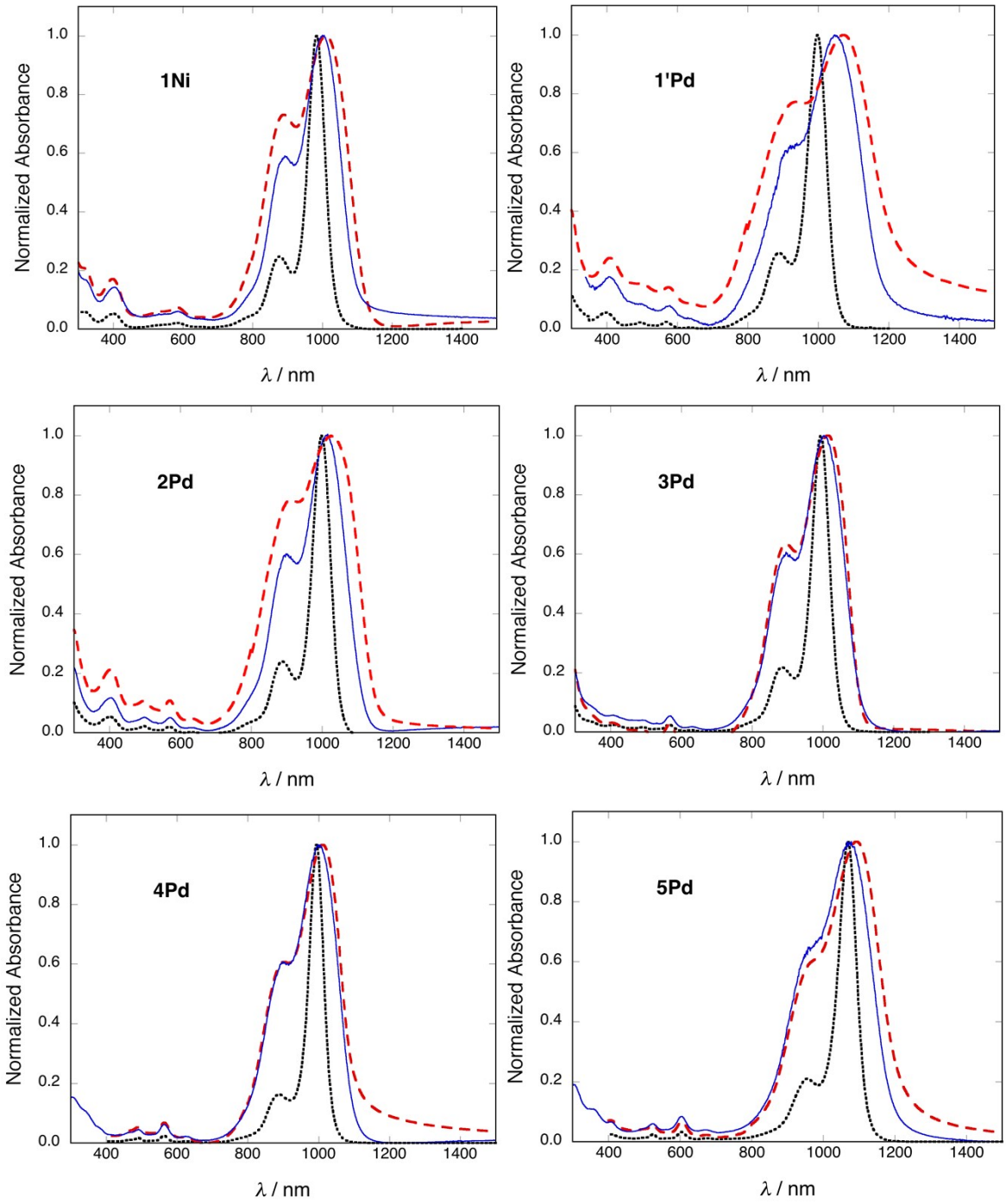

Figure S1. Top: UV-vis-NIR absorption spectra for *meso*-M(PPh_3)$_2$Cl dyes in dilute chloroform solution (black dotted line), in 50 wt% blends with APC (blue solid line), and in neat films (red dashed lines).

Table S1. Absorption Maxima for *meso*-M(PPh$_3$)$_2$Cl Dyes and their *meso*-Cl Precursors in CHCl$_3$.

M(PPh$_3$)$_2$Cl dye	λ_{max}(M(PPh$_3$)$_2$Cl dye) / nm (ν_{max} / 10^3 cm^{-1}) [ε_{max} / 10^5 M^{-1} cm^{-1}]	λ_{max}(Cl precursor) / nm (ν_{max} / 10^3 cm^{-1})	$\Delta\nu_{max}$ on metallation, / 10^3 cm^{-1}
1Ni	984 (10.16) [3.1]	1063 (9.41)	–0.75
1Pd	999 (10.01) [3.6]	1063 (9.41)	–0.60
1'Pd	999 (10.01)	1063 (9.41)	–0.60
2Pd	999 (10.01) [3.5]	1063 (9.41)	–0.60
3Pd	995 (10.05) [3.5]	1054 (9.49)	–0.56
4Pd	994 (10.06) [3.4]	1051 (9.52)	–0.55
5Pd	1069 (9.35) [3.3]	1142 (8.76)	–0.60

3. Thermogravimetric Analysis (TGA) Data

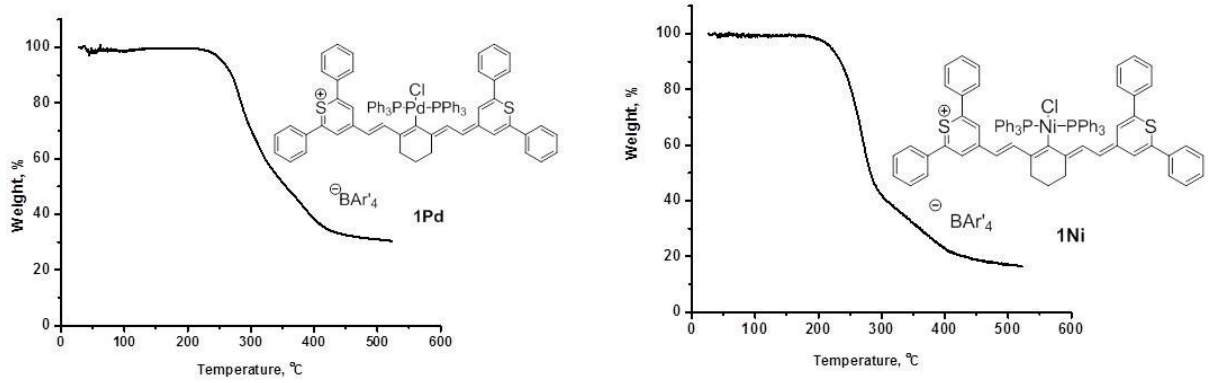

Figure S2. Thermogravimetric analysis (5 °C min–1, Supporting Information) reveals onsets of weight loss at 240 and 185 °C for **1Pd** and **1Ni**, respectively.

4. Quantum-Chemical Calculations

4.1. Theoretical Methodology

Electronic Structure Calculations. Geometry optimisations were performed using Density Functional Theory (DFT) with the long-range corrected ωB97X-D functional[7,8] with the default range separation parameter (ω = 0.2 Bohr^{-1}) and the cc-pVDZ basis set.[9] The cc-pVDZ basis sets for the Ni, Pd, and Pt metals were taken from the EMSL Basis Set Exchange.[10,11] For comparison with experiment, the optimisations were conducted using the Polarisable Continuum Model (PCM) to model chloroform (ε = 4.7113). The absence of imaginary frequencies confirmed the geometries obtained represented global

minima. Symmetry-Adapted Cluster Configuration Interaction (SAC-CI)[12, 13] calculations, with chloroform as the implicit dielectric medium, were used to obtain the vertical excited-state energies, transition dipole moments, and state dipole moments; since the SAC-CI active space incorporates single and higher-order excitations, it can correctly describe two-photon absorbing states, which is essential to accurately capture the molecular third-order NLO properties. The chosen active space included the 40 highest-lying occupied orbitals and the 110 lowest-lying unoccupied orbitals, which were obtained at the Hartree-Fock/cc-pVDZ level of theory. The third-order polarisabilities, $\gamma(\omega;\omega,-\omega,\omega)$, were obtained by a sum-over-states perturbation approach using the SAC-CI results as inputs for an essential-state calculation involving 10 excited states. All electronic-structure calculations were performed in the Gaussian 09 (Rev. D.01) suite of programs.[14]

Molecular Dynamics Simulations of Amorphous Structures. The molecular dynamics simulations and subsequent analyses of the polymethine-polymethine and polymethine-counterion geometries were conducted as in our previous work.[15,16] In brief, the GROMACS 4.5.4 package[17] was used to conduct atomistic molecular dynamics (MD) simulations using the OPLS-AA force field.[18] This force field has previously shown good agreement with experiment for polymethine aggregates in solution.[19] The initial geometries of the isolated polymethines and counterions were obtained using the same level of theory without PCM as detailed above, with the atomic charges used in the MD simulations obtained from NBO calculations likewise at the same level theory. Since *cis-trans* isomerisation of the polymethine chains is not expected to occur in films, all torsions about the C-C bonds in the polymethine backbone were constrained to within 10° of planarity to prevent isomerisation during the high-temperature annealing. After generating an initial geometry by randomly placing polymethines and counterions in a periodic box, the energy was minimised at constant volume, and an initial run of 10 ps was performed at 50 K under the NVT ensemble. Following the initial run, the simulation box was equilibrated at 800 K under the NPT ensemble using the Berendsen barostat until the volume equilibrated, and then allowed to run for several additional ns. Several geometries at 1 ns intervals were extracted, and this series of amorphous geometries were equilibrated for 1 ns at the annealing temperature using the Parrinello-Rahman barostat, cooled over 2 ns to 300 K, and finally simulated for 1 ns at 300 K. The following analyses used the final 1 ns of this simulation. The Nose-Hoover thermostat and periodic boundary conditions were used for all simulations, along with a time step of 1 fs; the Ewald summation as used for Coulomb interactions and the spherical cutoff for the summation of van der Waals interactions was set a 1.0 nm. The results were averaged over enough simulations to obtain a total of at least 1200 polymethine-counterion pairs. Details concerning the analysis of the simulation results are discussed in section 4.3.

4.2. Theoretical Results: Geometric and Electronic Structure, and Optical Properties

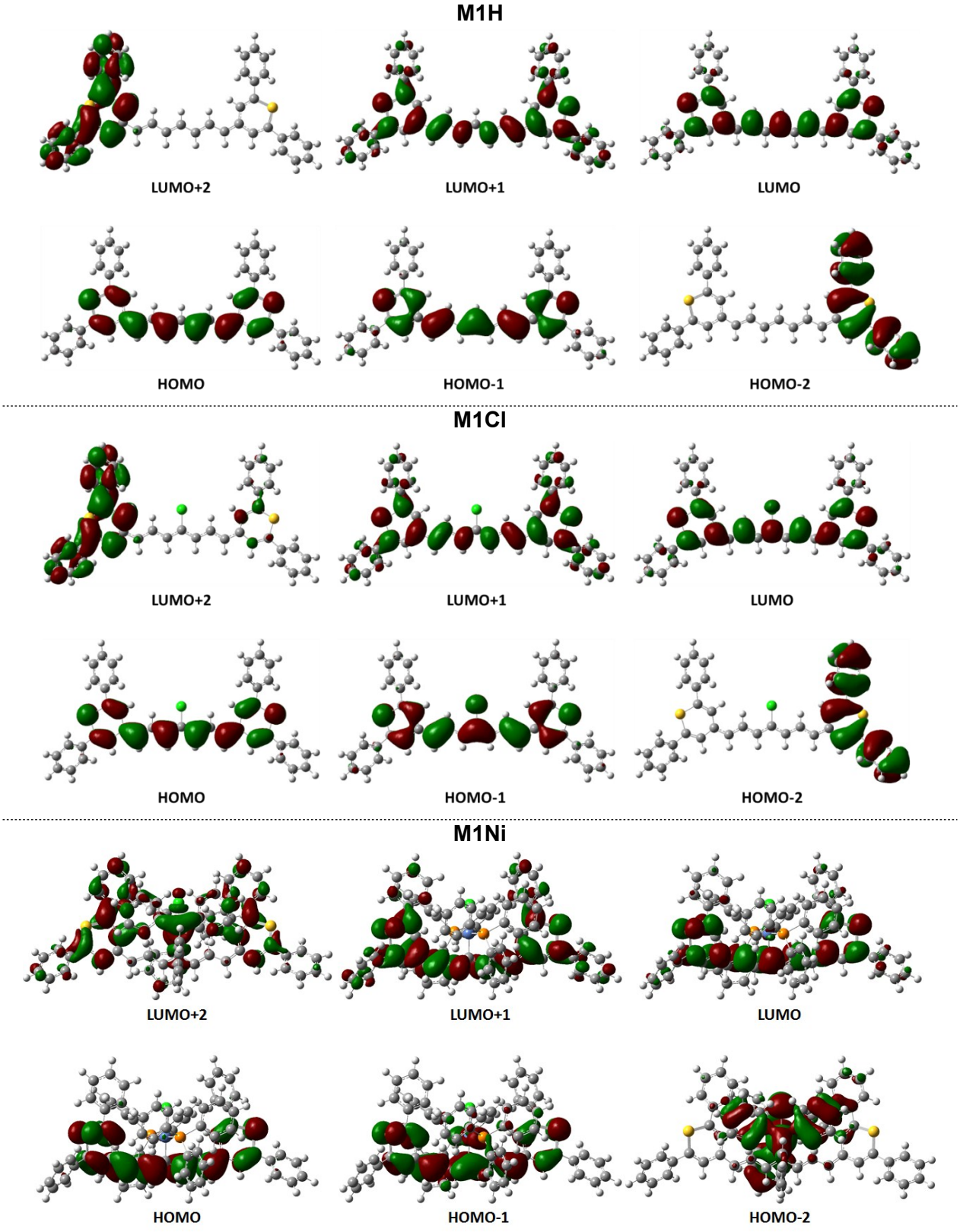

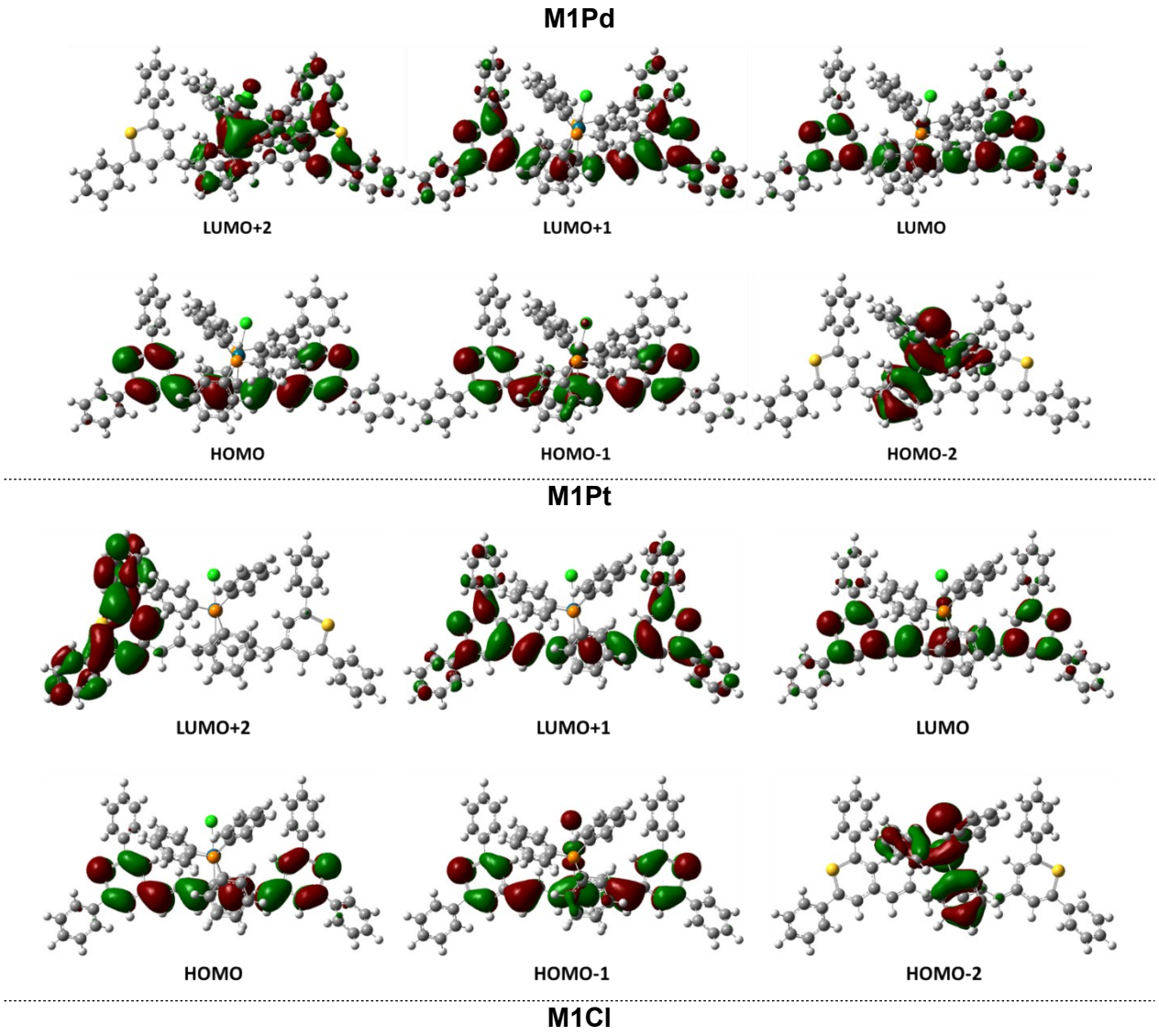

Figure S3. Frontier molecular orbitals for the model polymethine cations shown in Chart 1 in implicit solvent at the ωB97X-D/cc-pVDZ level of theory.

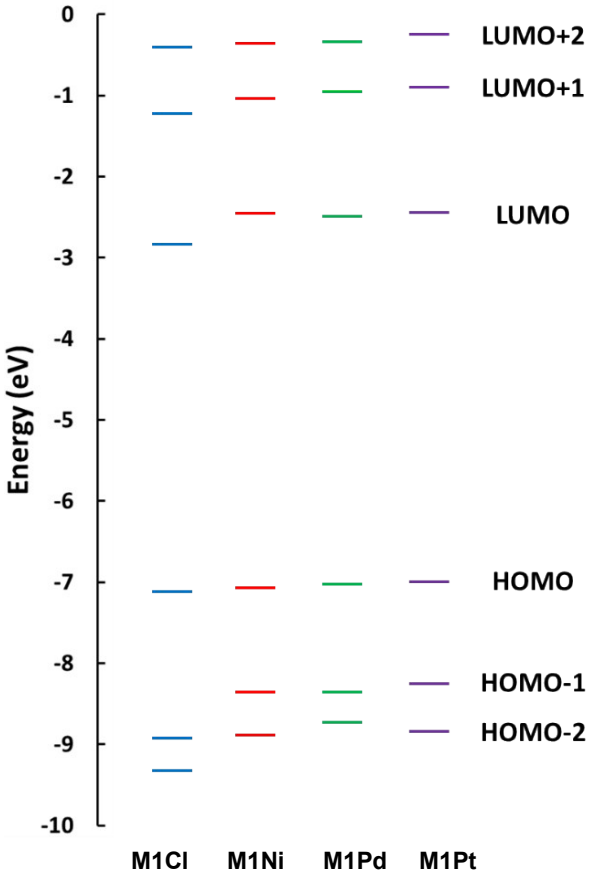

Figure S4. Energies of frontier molecular orbitals for model polymethine cations in implicit solvent at the ωB97X-D/cc-pVDZ level of theory.

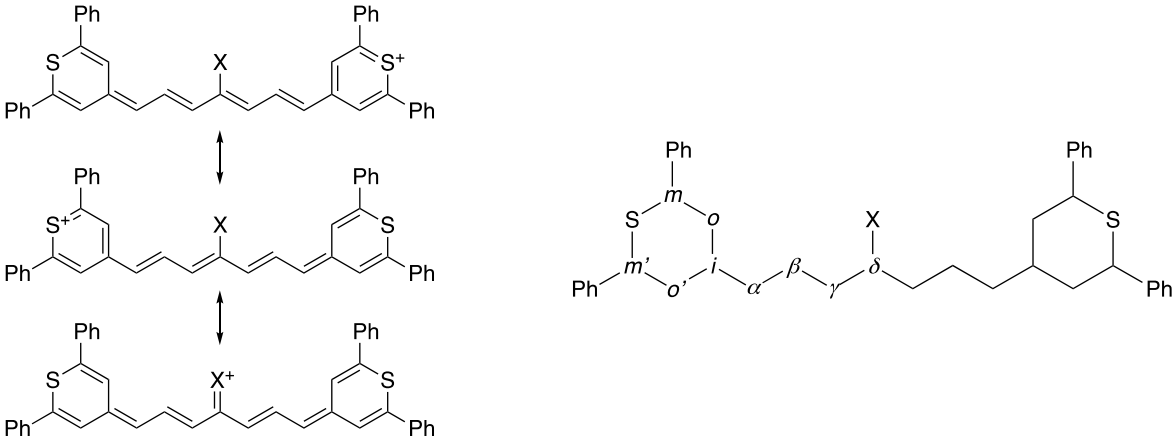

Figure S5. Left: resonance structures for model compounds; the bottom structure represents π-donation by the *meso*-substituent, X. Right: atom labeling used in Table S2.

Table S2. Selected Bond Lengths (Å) from ωB97XD/cc-pVDZ Geometries for Model Polymethine Cations in $CHCl_3$.[a]

Bond	**M1Cl**	**M1Ni**	**M1Pd**	**M1Pt**
S—C_m	1.74	1.75	1.75	1.75
S—$C_{m'}$	1.74	1.75	1.75	1.75
C_m—C_o	1.36	1.36	1.35	1.36
$C_{m'}$—$C_{o'}$	1.36	1.36	1.36	1.36
C_o—C_i	1.43	1.44	1.45	1.44
$C_{o'}$—C_i	1.44	1.44	1.44	1.44
C_i—C_α	1.43	1.44	1.45	1.44
C_α—C_β	1.39	1.41	1.41	1.41
C_β—C_γ	1.39	1.38	1.38	1.38
C_γ—C_δ	1.40	1.42	1.41	1.42
C_δ—X	1.75	1.90	2.01	2.01

[a]See Figure S5 for definitions of atom labels.

Table S3. SAC-CI/HF/cc-pVDZ-Calculated Vertical Excitation Energies (*E*), Transition Dipole Moments (μ), and CI Description for Low-Lying Excited States of Model Polymethine Cations in $CHCl_3$.[a]

	M1Cl	**M1Ni**	**M1Pd**	**M1Pt**
E_{ge} (μ_{ge}),	1.62 (22.39)	2.61 (17.39)	2.57 (18.38)	2.59 (18.64)
CI composition	0.92| H→L⟩	0.95| H→L⟩	0.95| H→L⟩	0.95| H→L⟩
$E_{ge'}$ ($\mu_{ee'}$),	3.28 (14.93)	3.59 (13.35)	4.52 (14.45)	4.54 (15.57)
CI composition	–0.53| H–1→L⟩	0.60| H–1→L⟩	–0.66| H–1→L⟩	0.66| H–1→L⟩
	–0.49| H→L+1⟩	–0.42| H→L+1⟩	0.59| H→L+1⟩	–0.57| H→L+1⟩
	–0.52| H,H→L,L⟩	–0.53| H,H→L,L⟩	0.30| H,H→L,L⟩	–0.33| H,H→L,L⟩
$E_{ge''}$ ($\mu_{ee''}$),		4.47 (16.94)		
CI composition		–0.68| H–1→L⟩		
		–0.59| H→L+1⟩		
		0.26| H,H→L,L⟩		

[a]Subscripts g, e, e', and e'' denote ground state, lowest lying 1PA-allowed excited state (S_1), lowest lying 2PA-allowed excited state (S_2), and (for **M1Ni**) second lowest 2PA-allowed excited state (S_3).

Table S4. Sum-Over-States Values of the Static Third-Order Polarisability, Re(γ_0), from SAC-CI/HF/cc-pVDZ-Calculations, and Decomposition into "N", "D", and "T" Contributions (10^{-33} esu), for Model Polymethine Cations in implicit $CHCl_3$.

	total	"N"-term	"D"-term	"T"-term
M1Cl	–29.9	–68.2	0.14	38.1
M1Ni	0.14	–5.97	0.02	6.08
M1Pd	–4.54	–7.79	0.19	3.07
M1Pt	–4.61	–8.04	0.01	3.42

4.3. Theoretical Results: Molecular Dynamics

Thiopyrylium-Counterion Geometries. First we examined the effect of $M(PPh_3)_2Cl$ substitution on the counterion position. An internal coordinate system was defined to analyze the thiopyrylium-counterion geometries. The origin C was defined as the geometric center of the two sulfur atoms. Vector X was computed as the normalised vector from C to the first terminal sulfur atom. Vector Y was computed as the negative of the normalised component of a vector from C to the location of the central carbon atom (C_δ) and, thus, orthogonal to X. The cross product of X and Y defined vector Z. Vector D was defined as the vector from C to the central atom of the counter anion. The displacements along the internal axes (D_x, D_y, D_z) were computed as the dot products of D with X, Y, and Z. The cutoff distance for polymethine-counterion pairs was set at –20 Å to 20 Å along each axis and each pair within this cutoff was considered and sorted into bins with a width of 1 Å in each direction. For each simulation, the analysis was conducted for 501 frames at 2 ps intervals and the results averaged. The bulk density of the thiopyrylium-counterion pairs was calculated as the product of the number of thiopyryliums and the number of counterions in each frame divided by the average frame volume. Each bin was normalised by dividing its count by the bin volume and the by the bulk density. Each X-Y displacement plot was constructed by averaging over a depth ranging from -5 Å to +5 Å along the z axis. Plots for **M1H-BF_4**, **M1H-BAr'_4**, and **M1Pd-Cl** are shown in Figure S6, which shows that, even using a small chloride counterion, the $Pd(PPh_3)_2Cl$ substituent effectively prevents close approach of the counterion to the center of the **M1Pd** cation, whereas even the larger BF_4 and BAr'_4 anions can approach the center of the **M1H** cation.

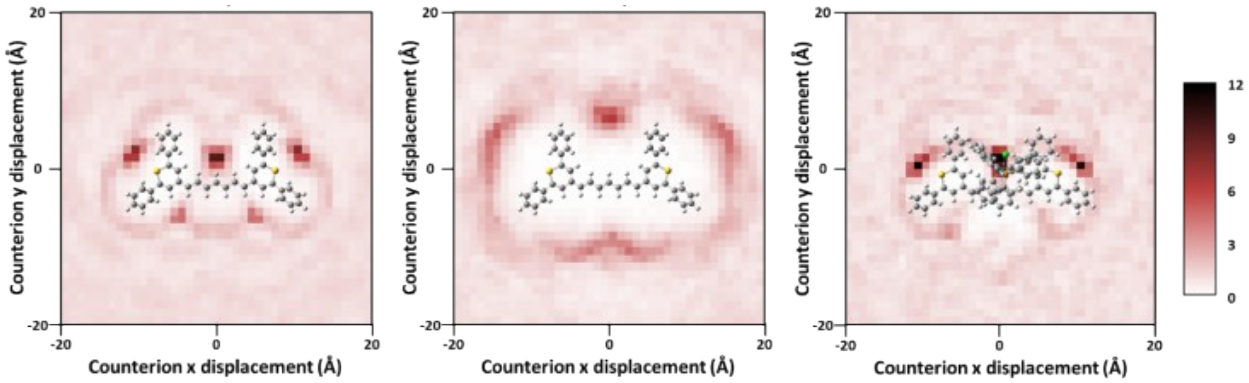

Figure S6. Counterion probability distribution from bulk MD simulations of **M1H-BF$_4$** (left), **M1H-BAr'$_4$** (center), and **M1Pd-Cl** (right). The color scale, far right, corresponds to the probability of finding thiopyrylium-counterion pairs at the displacement in question, with the probability of 1 corresponding to the average bulk density of polymethine-counterion pairs. Note the dark spot in the center of the plot for **M1Pd-Cl** does not refer to the Cl^- anion, but to the chlorine atom of the $Pd(PPh_3)_2Cl$ moiety.

Thiopyrylium-Thiopyrylium Aggregate Geometries. The positions of the C_i carbon atoms (Figure S5) were used to analyze the thiopyrylium-thiopyrylium aggregate geometries (Figure S7). For each pair of yes (A and B), vectors A and B were defined by between the two terminal atoms, while the geometric centers of the dyes, C_A and C_B, were computed as the average positions of the two terminal backbone atoms, and vector C was defined as the vector between C_A and C_B. Vector F, the offset, is the projection of C onto A, and vector R, the radial distance, is the projection of C into the plane perpendicular to A. The offset and the radial distance were computed as the magnitudes of vectors F and R, respectively. The torsion angle was computed by determining vector B' as the projection of B into the plane perpendicular to R, then computing the angle (D) between A and B'. Since the two ends of the dye are identical, the torsion angle was computed as (180°–D) if D was greater than 90°. All ordered pairs of dyes were considered, as the offset, radial distance, and torsion and depend on whether dye A or B is chosen first. All thiopyrylium pairs within a radial distance of 6 Å and an offset less than 12 Å were considered and sorted in bins of 1 Å offset and 10° torsion angle. Each bin count was normalised relative to the bulk density. The analysis was conducted for each simulation over 501 frames at 2 ps intervals and then averaged.

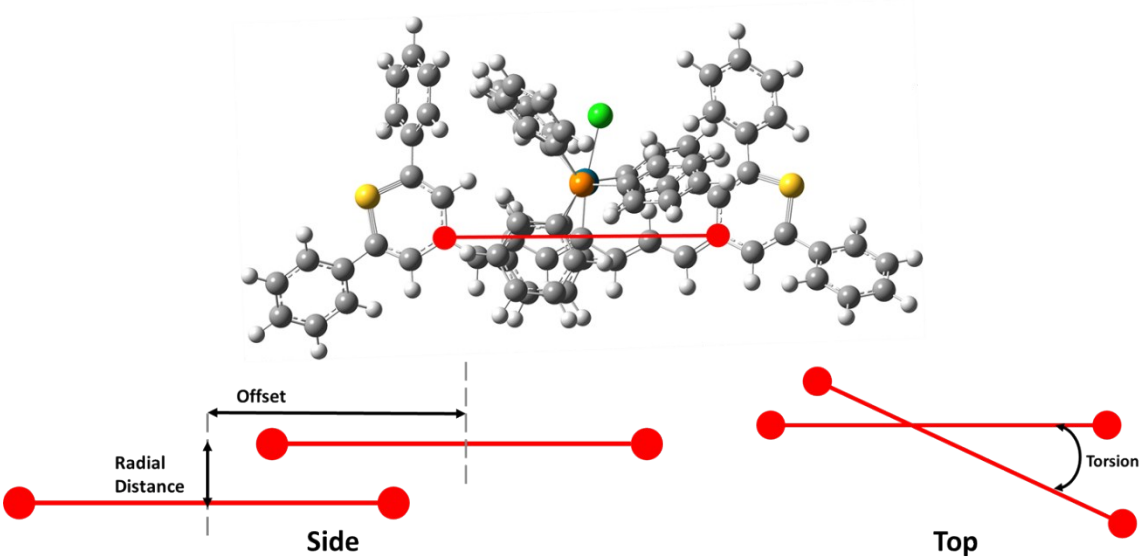

Figure S7. Atoms selected for analysis of thiopyrylium aggregate geometries (top) and definition of the offset and torsion used to represent thiopyrylium-thiopyrylium geometries in Figure 4 (bottom).

5. Electrochemical Data

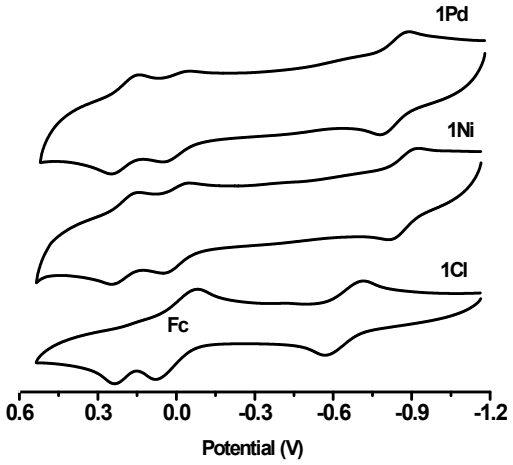

Figure S8. Cyclic voltammograms (beginning at –1.2 V) of **1Cl**, **1Ni**, and 1Pd in CH_2Cl_2 / 0.1 M Bu_4NPF_6 containing internal ferrocene (the reversible process for which is seen at 0 V and, in the voltammogram for **1Cl**, labeled "Fc").

6. Characterisation of NLO Properties

The third order nonlinear optical measurements were performed via dual-arm (DA) Z-Scan technique[20] which can improve the signal-to-noise ratio (SNR) by an order of magnitude compared to single arm Z-Scan.[21] In this method, the two arms are calibrated at a wavelength of 1.55 μm identically (e.g. pulse energy, beam waist, pulse width, and beam pointing, etc.) and the scans are simultaneously performed with solution in one arm and solvent in the other to eliminate correlated noise and subtract the effect of the solvent. The open-aperture (OA) signal for a 0.5 mm thick GaAs and close-aperture (CA) signal for a 1 mm thick fused silica samples are measured to find the spot size and relative pulsewidth in each arm. The details of the DA Z-Scan technique are reported in ref. 20. Figure S9a and b shows the normalised transmission of OA and CA/OA for **1Pd** and Figure S9c and d shows the normalised transmission of OA and CA/OA for **1Ni** for three different pulse energies. The measurement signals are fitted[21] to obtain two-photon absorption (2PA) from OA and negative nonlinear refraction (NLR) from CA/OA, respectively. Similar measurements were performed on a **5Pd** thin-film sample by having the substrate in one arm and the sample in the other. The real part of the third-order susceptibility, $\mathrm{Re}(\chi^{(3)}) = -3 \times 10^{-11}$ esu, and an upper limit for the imaginary part $\mathrm{Im}(\chi^{(3)}) \leq 2.8\times10^{-12}$ esu, are found by fitting the signals. For the solution the 2PA figure-of-merit (FOM) is $|\mathrm{Re}(\gamma)/\mathrm{Im}(\gamma)|$ and for the film is $|\mathrm{Re}(\chi^{(3)}/\mathrm{Im}(\chi^{(3)})|$.[22]

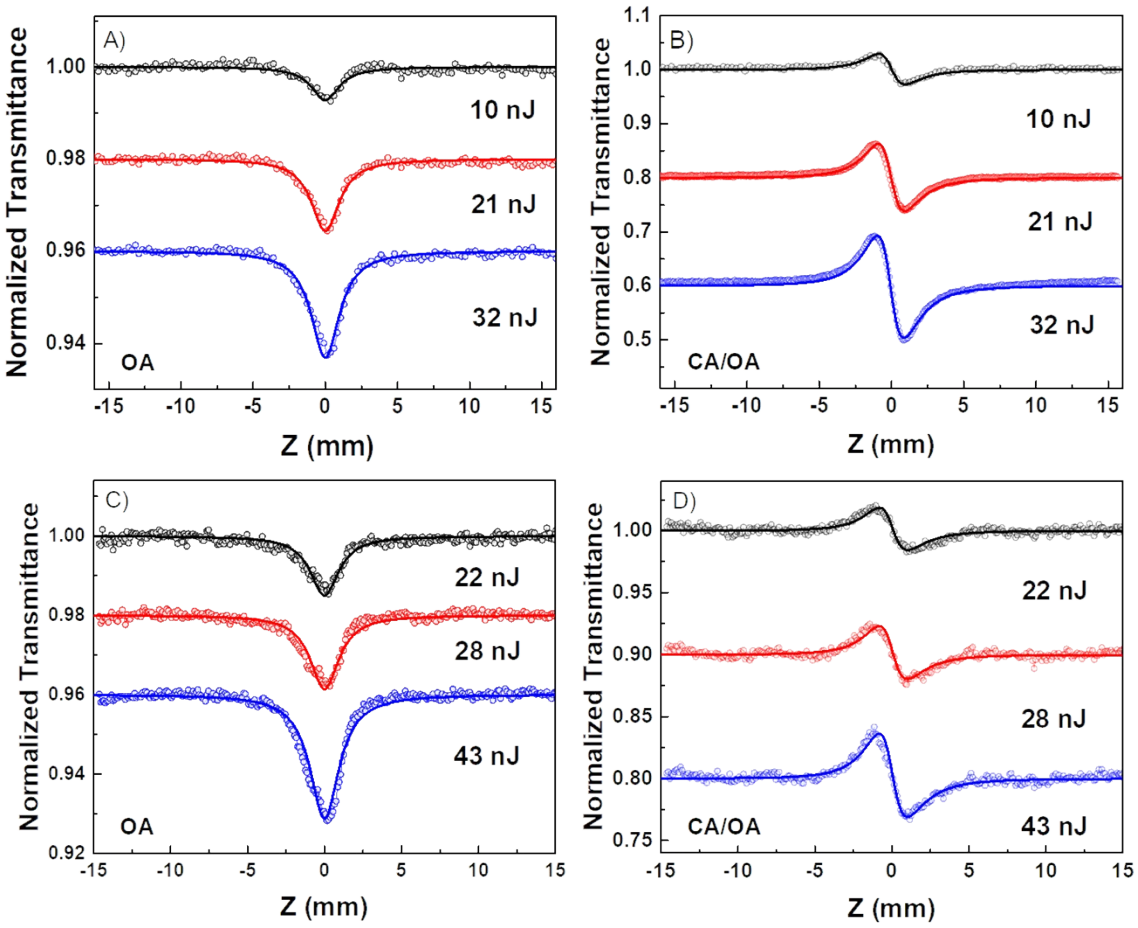

Figure S9. a) Open-aperture (OA) DA Z-Scans of a 5.7 mM solution of **1Pd** in chloroform. b) Closed-aperture (CA) signal divided by the OA signal for **1Pd**. c) OA DA Z-Scans of 9.3 mM solution of **1Ni** in chloroform. d) Closed-aperture (CA) signal divided by the OA signal for **1Ni** with three different pulse energies at a wavelength of 1.55 μm. Solid lines are the fits to the experimental data. The 2PA cross-section (δ_{2PA}) and the nonlinear refraction cross-section (δ_{NLR}) are deduced to be +140 GM and –786 GM for **1Pd**, respectively, which correspond to values of Re(γ) = -2.4×10^{-32} esu and Im(γ) = $+0.2\times10^{-32}$ esu.[22] Similarly, for **1Ni**, δ_{2PA} = +46 GM and δ_{NLR} = –134 GM, and the real and imaginary parts of the third-order polarisability -0.4×10^{-32} esu and $+0.06 \times 10^{-32}$ esu, respectively.[22]

7. Film Processing, UV-vis-NIR Absorption, and Linear Loss Measurements

APC Purification. APC pellets (Poly(bisphenol A carbonate) of average molecular weight ~45,000 g/mol by GPC, used as provided by Sigma Aldrich, Product # 181625) were dissolved in 1,1,2-trichloroethane at 75 °C to yield a ca. 12% wt solution, then precipitating in cold methanol with slow

stirring and then drying under vacuum filtration. This cycle was repeated several times and after the final precipitation the APC was dried in a vacuum oven for 12 h at 80 °C.

UV-vis-NIR Absorption Measurements. 50% wt APC:dye blend films for UV-vis-NIR measurements were made by combining equal masses of an 8% wt solution of each dye in 1,2-dichloroethane (DCE) and an 8% wt APC solution in DCE to make the 50% wt blend solution. After sufficient mixing, a 30 μL aliquot of the blend solution is dropped onto a clean (sonicated in acetone 10 min, then twice in methanol for 10 min each) 15 × 15 mm^2 microscope slide while the substrate is spinning at 8000 RPM in a spin coater. After dropping the aliquot, the film was left to spin to dryness at 8000 RPM for ca. 40 s. Film thicknesses were 170-340 nm. Absorption measurements were taken using a Shimadzu UV-3101PC UV-vis-NIR Spectrophotometer.

Linear Loss Measurements. 15 × 25 × 0.5 mm^3 fused silica (University Wafer) substrates were cleaned prior to film processing according to the recipe listed in the previous section. 50% wt blend solutions from DCE for linear loss were made according to the recipe listed in the previous section. Prior to spin coating, the blend solutions are filtered with a 0.2 μm PTFE membrane syringe filter (VWR 28145-505) directly onto the fused silica substrate so that the blend solution floods the entire surface. Solutions from DCE were spun at 500 rpm/s for 2 s then dried overnight under vacuum, protected from ambient light. 1Pd from DCE was spun under different conditions involving a slow acceleration step at 100 rpm/s for 5 s, followed by accelerating 250 rpm/s to 750 rpm and holding for 5 minutes at 750 rpm. The linear loss and refractive index of blend films at 1550 nm was characterised by a prism coupler (Metricon 2010), using a CW diode laser (Melles-Griot, 57STL051) with an output power of approximately 1.2 mW. The error of measured linear loss is estimated to be ±20%. Typical linear loss scan length was 2.5 cm. Thicknesses of each film were measured by a Dektak 6M stylus profilometer.

Table S5. Refractive Indices at 1550 nm and Thicknesses for 50% wt APC/Dye Films

Compound	Average Refractive Index	Thickness / μm
1Ni	---	---
1Pd	1.74	1.71
1'Pd	1.83	0.95
2Pd	1.76	0.95
3Pd	1.72	1.08
4Pd	1.71	0.96
5Pd	1.72	0.91

8. NMR Spectra for *meso*-Metallated Dyes

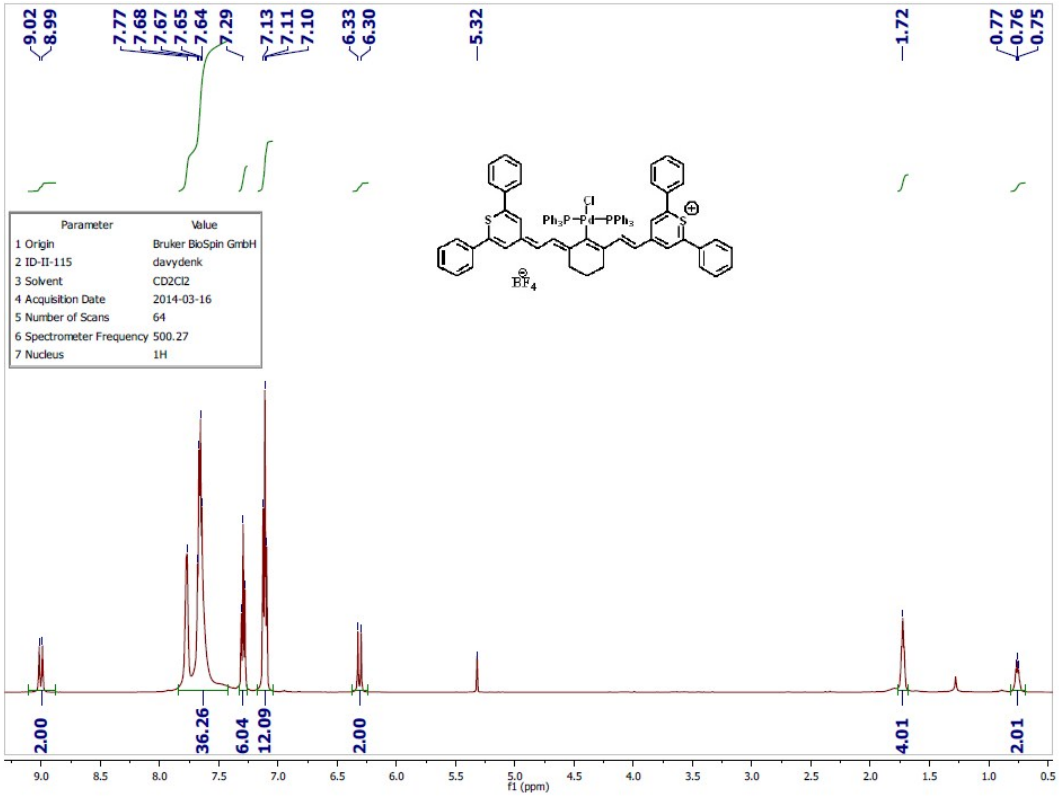

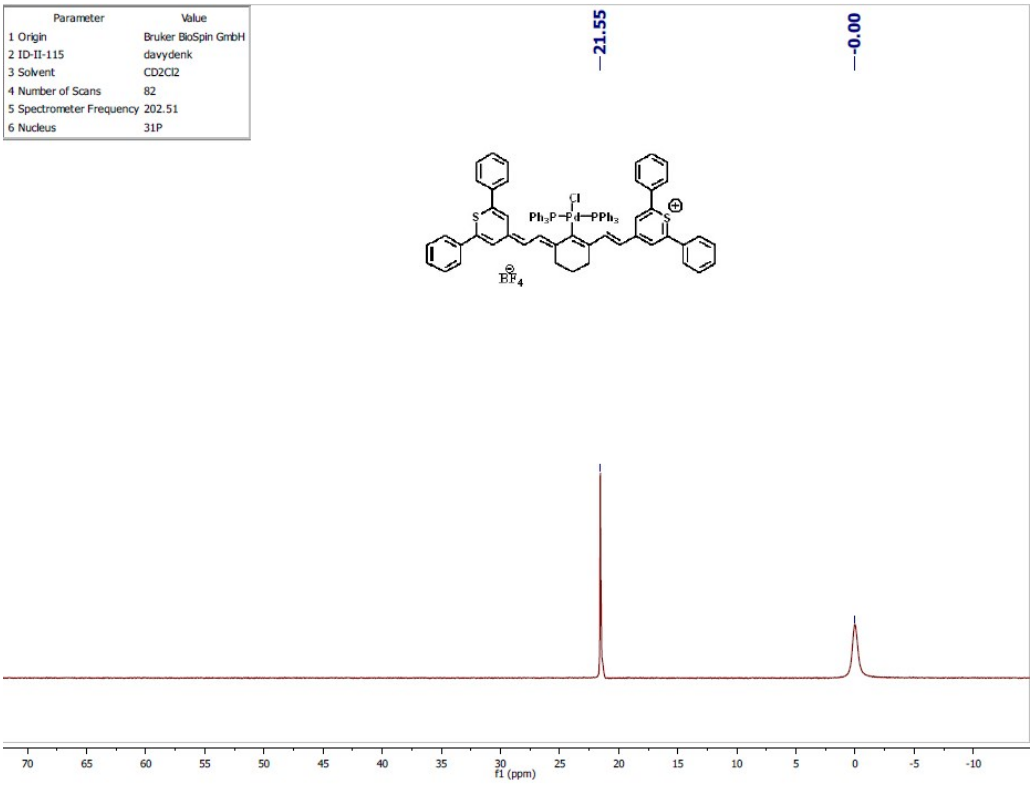

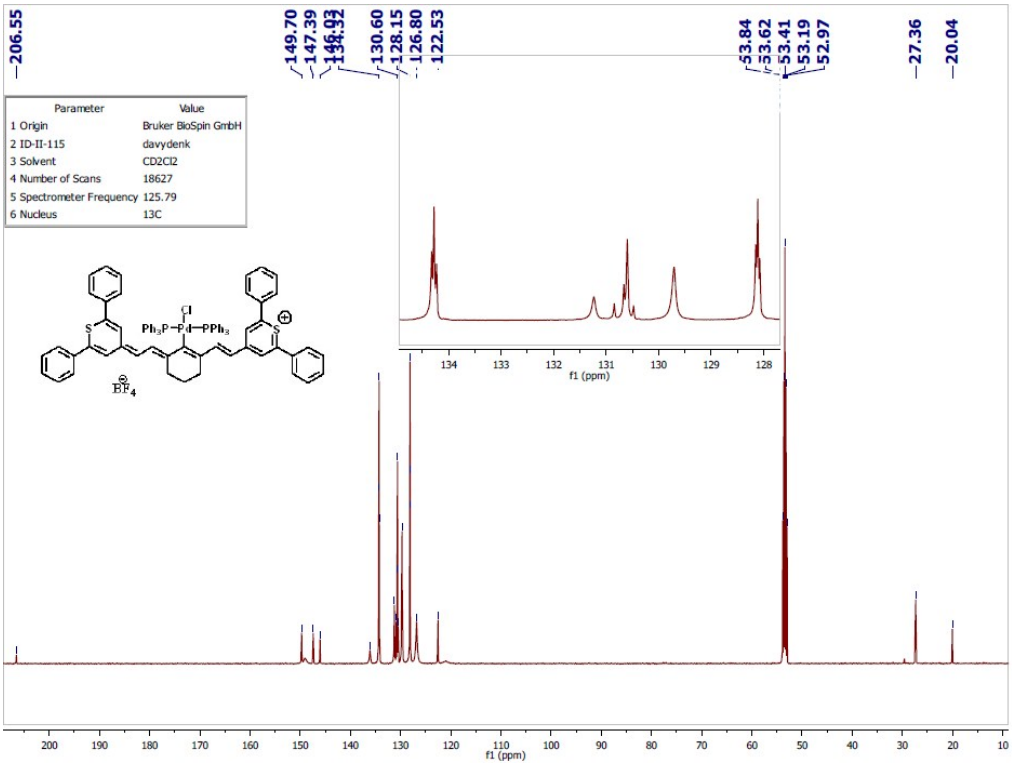
206.55
149.70
147.39
130.60
128.15
126.80
122.53
53.84
53.62
53.41
53.19
52.97
27.36
20.04
Parameter Value
1 Origin Bruker BioSpin GmbH
2 ID-II-115 davydenk
3 Solvent CD2Cl2
4 Number of Scans 18627
5 Spectrometer Frequency 125.79
6 Nucleus 13C
f1 (ppm)

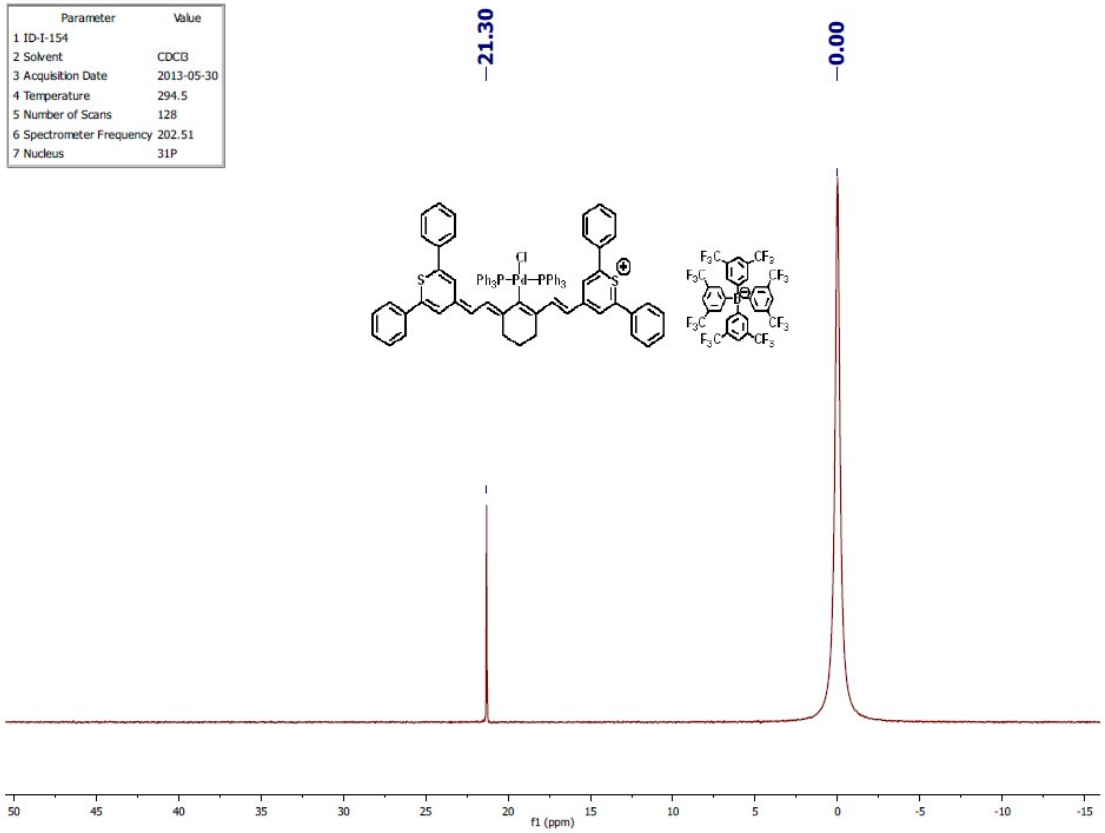
Parameter Value
1 ID-I-154
2 Solvent CDCl3
3 Acquisition Date 2013-05-30
4 Temperature 294.5
5 Number of Scans 128
6 Spectrometer Frequency 202.51
7 Nucleus 31P
21.30
0.00
f1 (ppm)

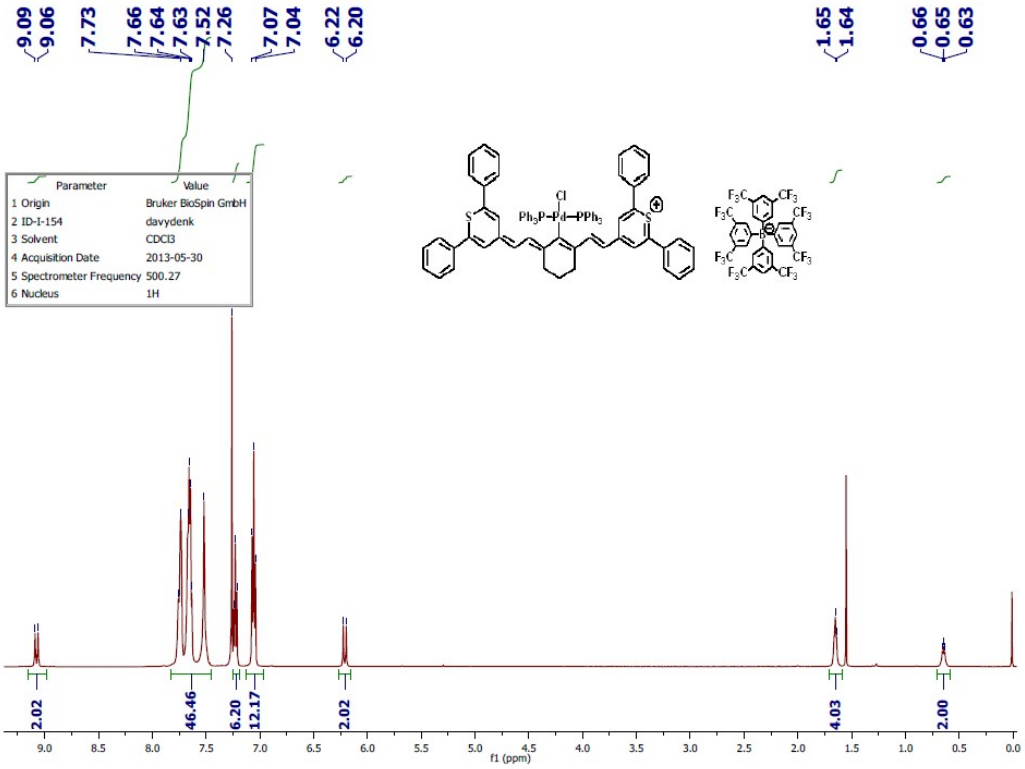
9.09
9.06
7.73
7.66
7.64
7.63
7.52
7.26
7.07
7.04
6.22
6.20
1.65
1.64
0.66
0.65
0.63
Parameter Value
1 Origin Bruker BioSpin GmbH
2 ID-I-154 davydenk
3 Solvent CDCl3
4 Acquisition Date 2013-05-30
5 Spectrometer Frequency 500.27
6 Nucleus 1H
2.02
46.46
6.20
12.17
2.02
4.03
2.00
f1 (ppm)

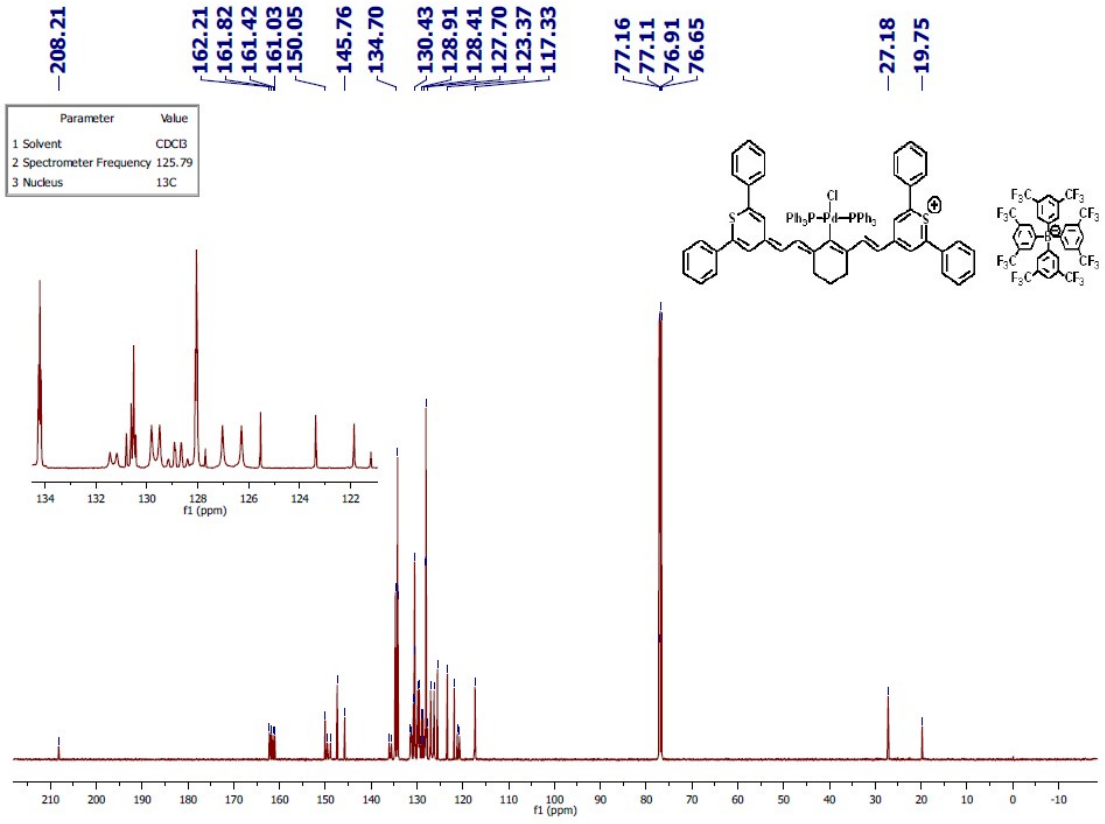
208.21
162.21
161.82
161.42
161.03
150.05
145.76
134.70
130.43
128.91
128.41
127.70
123.37
117.33
77.16
77.11
76.91
76.65
27.18
19.75
Parameter Value
1 Solvent CDCl3
2 Spectrometer Frequency 125.79
3 Nucleus 13C
f1 (ppm)

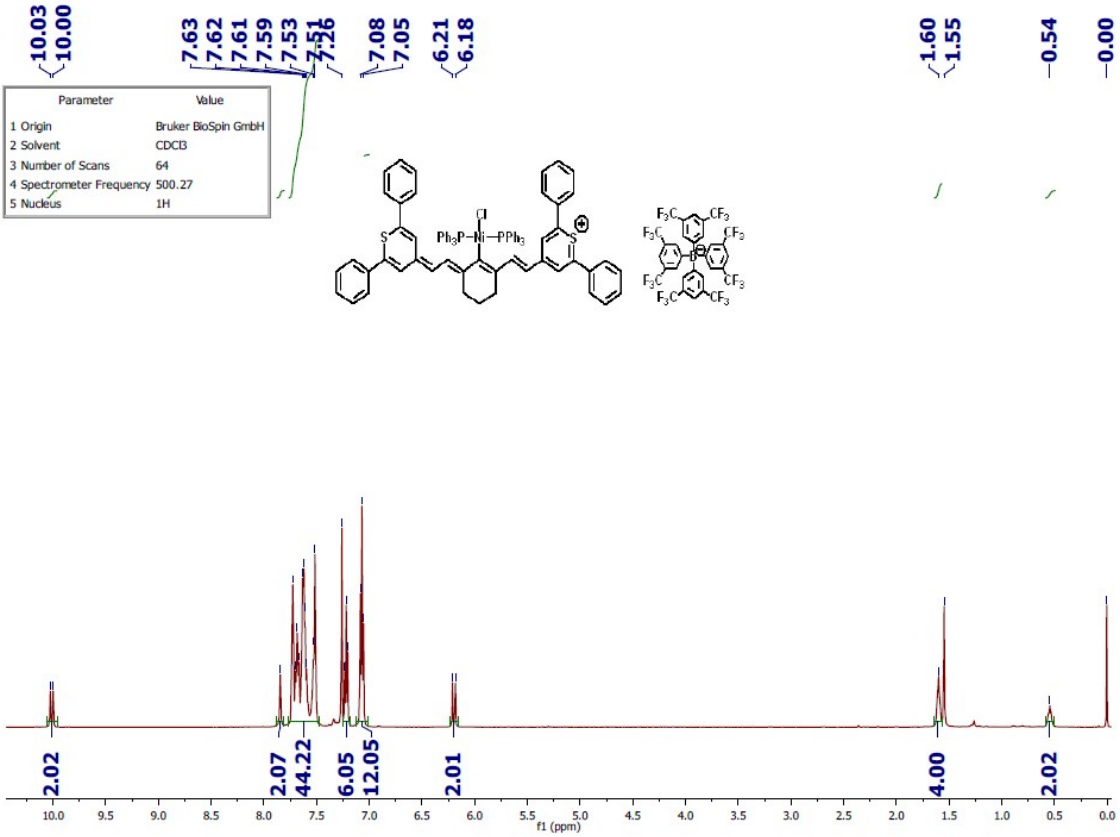
10.03
10.00
7.63
7.62
7.61
7.59
7.53
7.51
7.26
7.08
7.05
6.21
6.18
1.60
1.55
0.54
0.00
Parameter Value
1 Origin Bruker BioSpin GmbH
2 Solvent CDCl3
3 Number of Scans 64
4 Spectrometer Frequency 500.27
5 Nucleus 1H
Cl
Ph3P–Ni–PPh3
S
S
F3C
CF3
CF3
F3C
F3C
CF3
CF3
F3C
B

2.02
2.07
44.22
6.05
12.05
2.01
4.00
2.02
10.0 9.5 9.0 8.5 8.0 7.5 7.0 6.5 6.0 5.5 5.0 4.5 4.0 3.5 3.0 2.5 2.0 1.5 1.0 0.5 0.0
f1 (ppm)

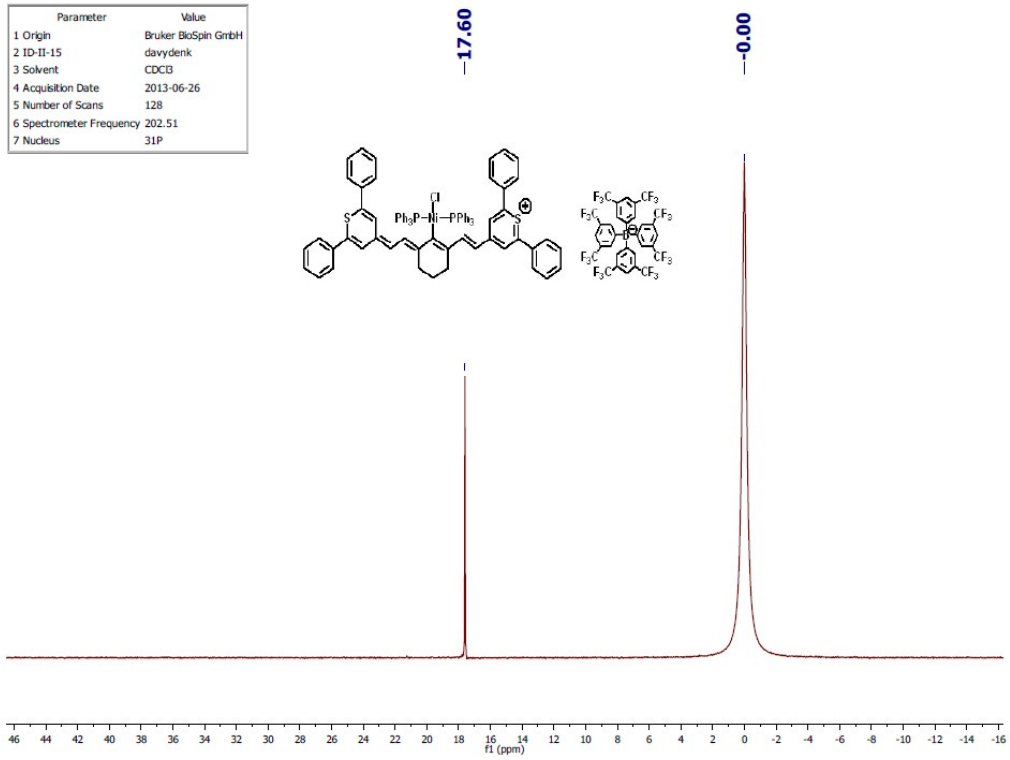
Parameter Value
1 Origin Bruker BioSpin GmbH
2 ID-II-15 davydenk
3 Solvent CDCl3
4 Acquisition Date 2013-06-26
5 Number of Scans 128
6 Spectrometer Frequency 202.51
7 Nucleus 31P
17.60
-0.00
Cl
Ph3P–Ni–PPh3
S
S
F3C
CF3
CF3
F3C
F3C
CF3
CF3
F3C
B
46 44 42 40 38 36 34 32 30 28 26 24 22 20 18 16 14 12 10 8 6 4 2 0 -2 -4 -6 -8 -10 -12 -14 -16
f1 (ppm)

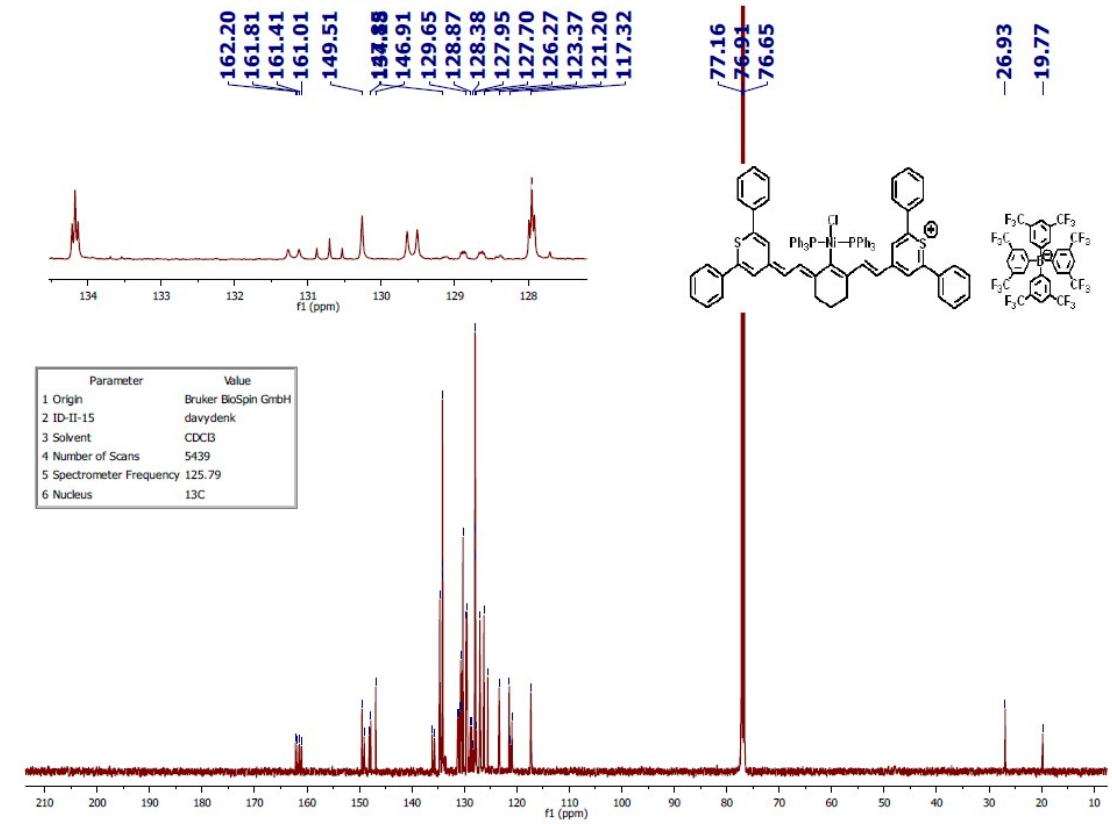
162.20
161.81
161.41
161.01
149.51
146.91
129.65
128.87
128.38
127.95
127.70
126.27
123.37
121.20
117.32
77.16
76.91
76.65
26.93
19.77
f1 (ppm)
Parameter Value
1 Origin Bruker BioSpin GmbH
2 ID-II-15 davydenk
3 Solvent CDCl3
4 Number of Scans 5439
5 Spectrometer Frequency 125.79
6 Nucleus 13C

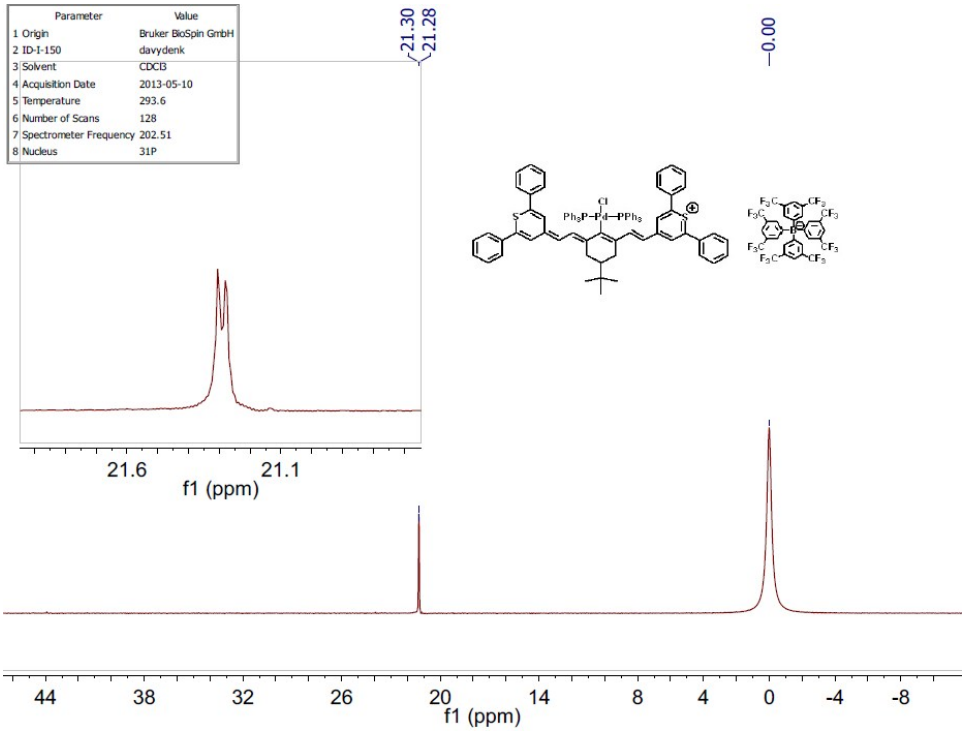
Parameter Value
1 Origin Bruker BioSpin GmbH
2 ID-I-150 davydenk
3 Solvent CDCl3
4 Acquisition Date 2013-05-10
5 Temperature 293.6
6 Number of Scans 128
7 Spectrometer Frequency 202.51
8 Nucleus 31P
21.30
21.28
0.00
f1 (ppm)

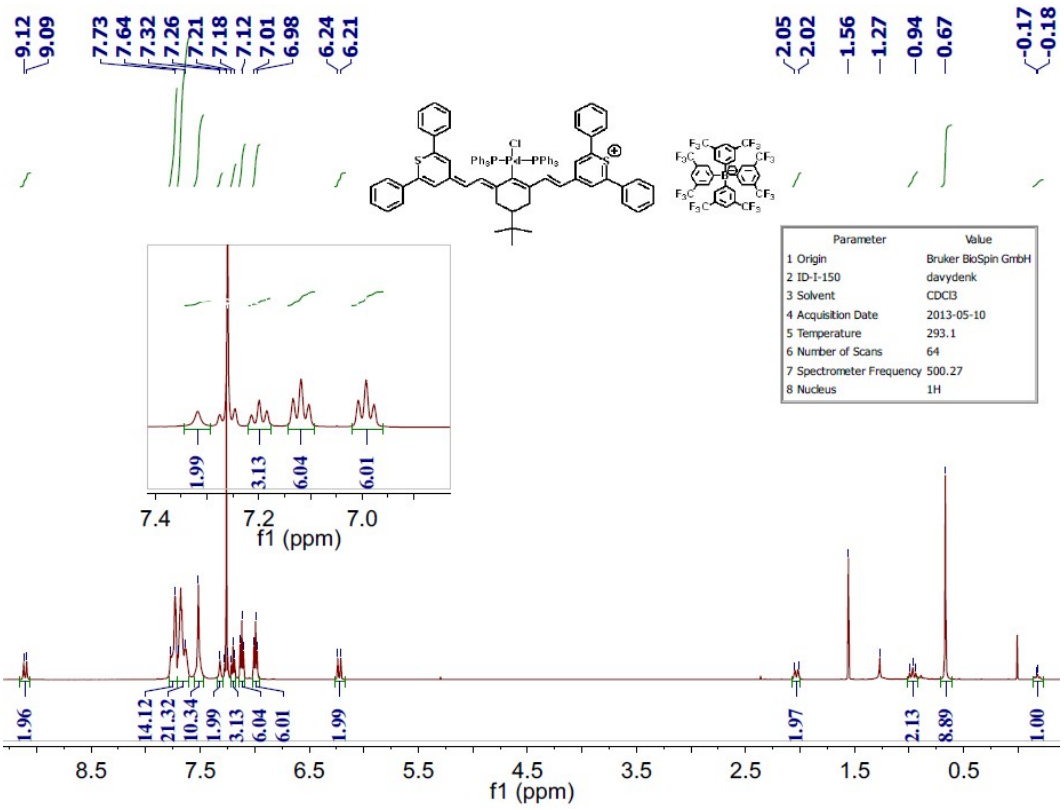
9.12
9.09
7.73
7.64
7.32
7.26
7.21
7.18
7.12
7.01
6.98
6.24
6.21
2.05
2.02
1.56
1.27
0.94
0.67
-0.17
-0.18
Parameter Value
1 Origin Bruker BioSpin GmbH
2 ID-I-150 davydenk
3 Solvent CDCl3
4 Acquisition Date 2013-05-10
5 Temperature 293.1
6 Number of Scans 64
7 Spectrometer Frequency 500.27
8 Nucleus 1H
1.99
3.13
6.04
6.01
7.4
7.2
7.0
f1 (ppm)
1.96
14.12
21.32
10.34
1.99
3.13
6.04
6.01
1.99
1.97
2.13
8.89
1.00
8.5
7.5
6.5
5.5
4.5
3.5
2.5
1.5
0.5
f1 (ppm)

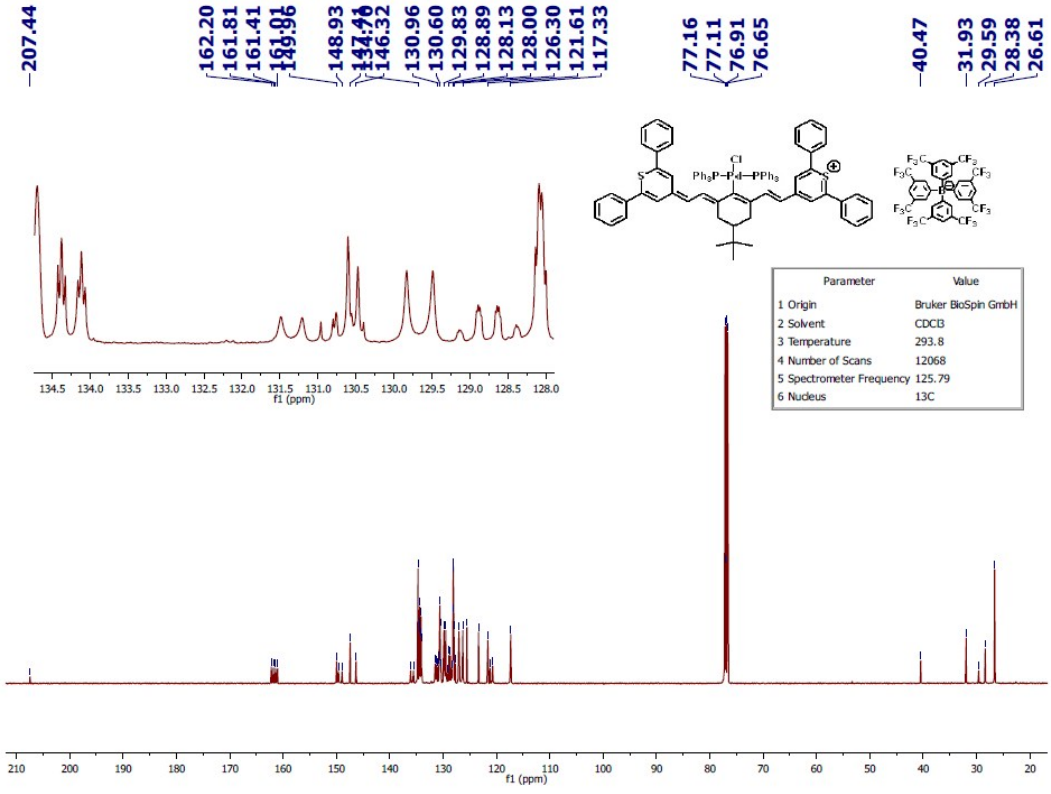
207.44
162.20
161.81
161.41
148.93
146.32
130.96
130.60
129.83
128.89
128.13
128.00
126.30
121.61
117.33
77.16
77.11
76.91
76.65
40.47
31.93
29.59
28.38
26.61
Parameter Value
1 Origin Bruker BioSpin GmbH
2 Solvent CDCl3
3 Temperature 293.8
4 Number of Scans 12068
5 Spectrometer Frequency 125.79
6 Nucleus 13C
134.5
134.0
133.5
133.0
132.5
132.0
131.5
131.0
130.5
130.0
129.5
129.0
128.5
128.0
f1 (ppm)
210
200
190
180
170
160
150
140
130
120
110
100
90
80
70
60
50
40
30
20
f1 (ppm)

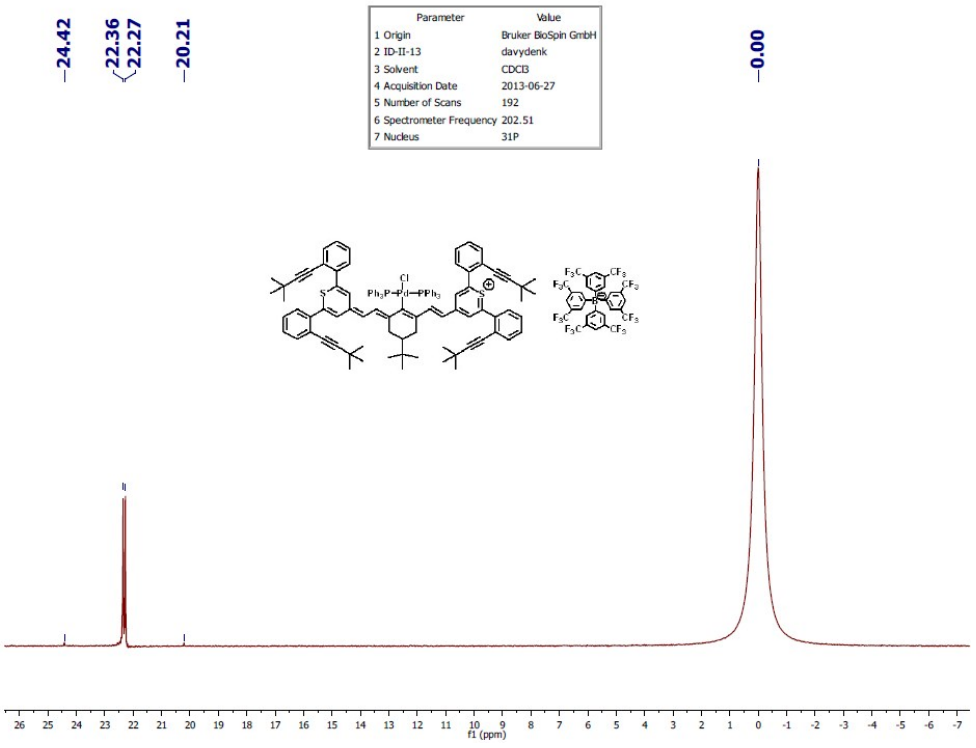
24.42
22.36
22.27
20.21
0.00
Parameter Value
1 Origin Bruker BioSpin GmbH
2 ID-II-13 davydenk
3 Solvent CDCl3
4 Acquisition Date 2013-06-27
5 Number of Scans 192
6 Spectrometer Frequency 202.51
7 Nucleus 31P
f1 (ppm)

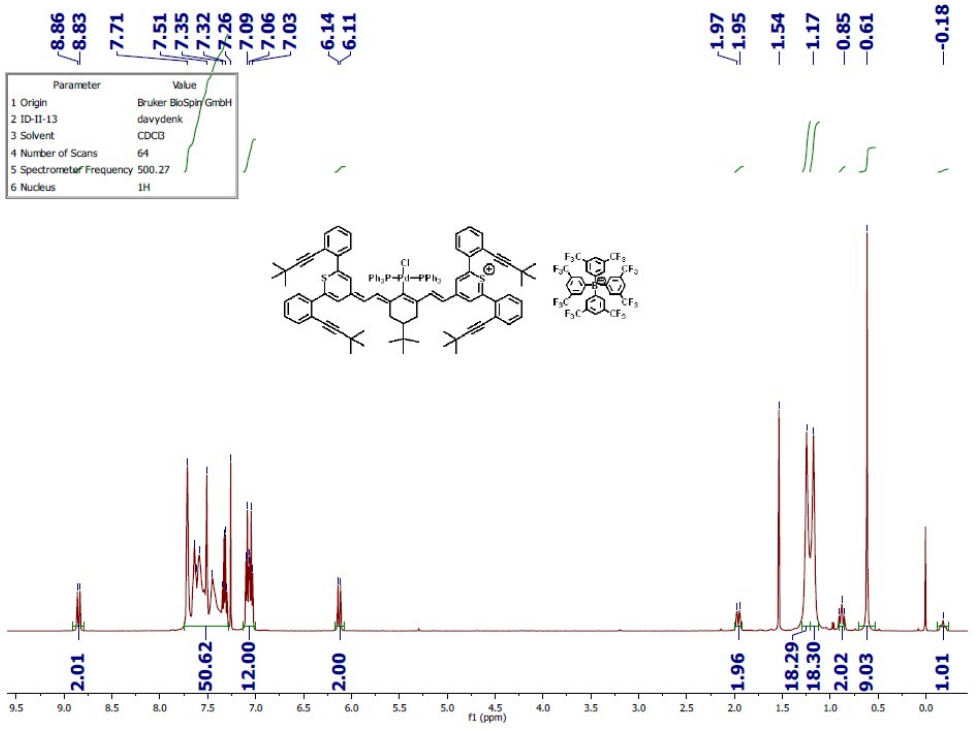
8.86
8.83
7.71
7.51
7.35
7.32
7.26
7.09
7.06
7.03
6.14
6.11
1.97
1.95
1.54
1.17
0.85
0.61
0.18
Parameter Value
1 Origin Bruker BioSpin GmbH
2 ID-II-13 davydenk
3 Solvent CDCl3
4 Number of Scans 64
5 Spectrometer Frequency 500.27
6 Nucleus 1H
2.01
50.62
12.00
2.00
1.96
18.29
18.30
2.02
9.03
1.01
f1 (ppm)

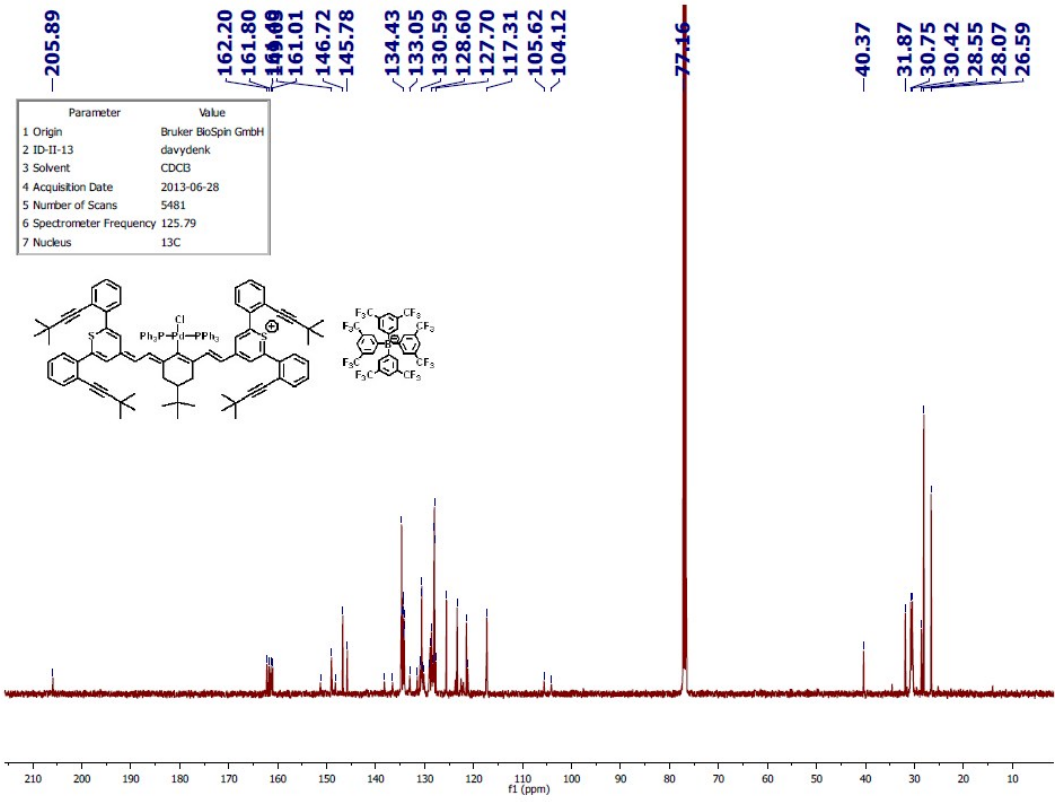
205.89
162.20
161.80
161.01
146.72
145.78
134.43
133.05
130.59
128.60
127.70
117.31
105.62
104.12
77.16
40.37
31.87
30.75
30.42
28.55
28.07
26.59
Parameter Value
1 Origin Bruker BioSpin GmbH
2 ID-II-13 davydenk
3 Solvent CDCl3
4 Acquisition Date 2013-06-28
5 Number of Scans 5481
6 Spectrometer Frequency 125.79
7 Nucleus 13C
f1 (ppm)

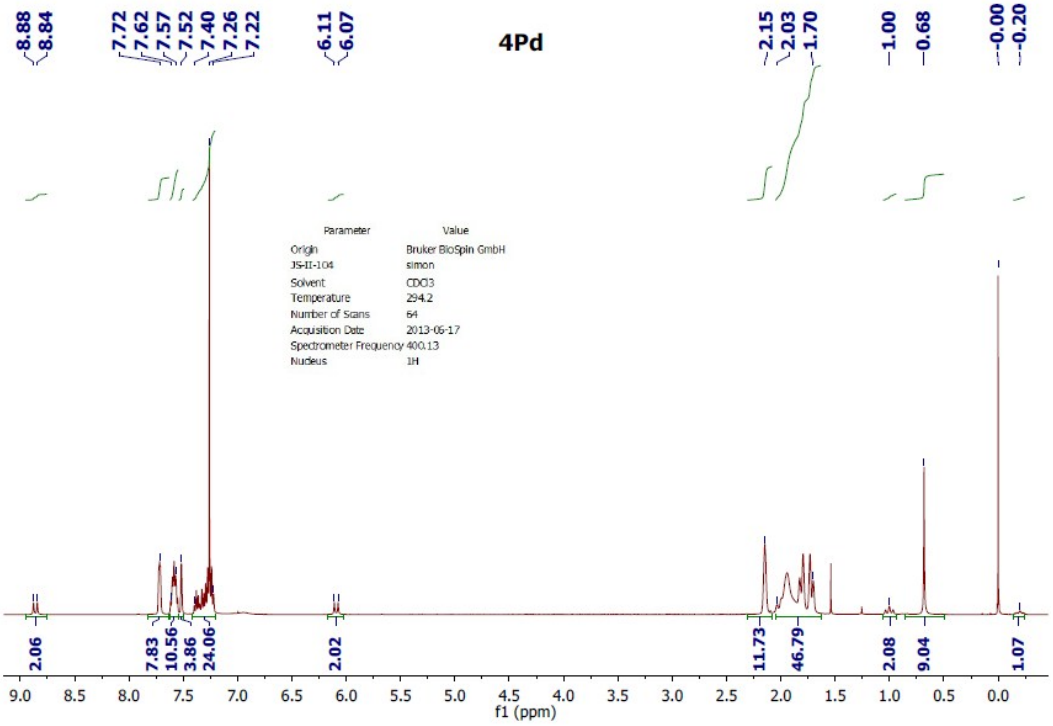
8.88
8.84
7.72
7.62
7.57
7.52
7.40
7.26
7.22
6.11
6.07
4Pd
2.15
2.03
1.70
1.00
0.68
-0.00
-0.20
Parameter Value
Origin Bruker BioSpin GmbH
JS-II-104 simon
Solvent CDCl3
Temperature 294.2
Number of Scans 64
Acquisition Date 2013-05-17
Spectrometer Frequency 400.13
Nucleus 1H
2.06
7.83
10.56
3.86
24.06
2.02
11.73
46.79
2.08
9.04
1.07
f1 (ppm)

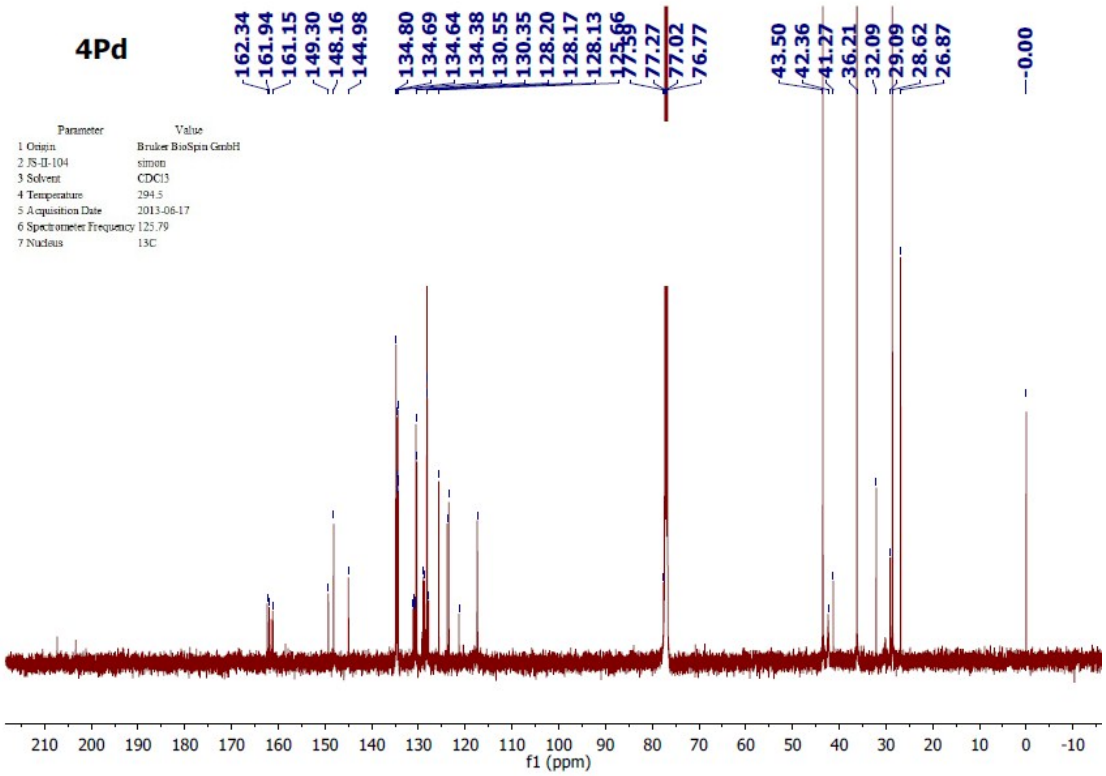
4Pd
162.34
161.94
161.15
149.30
148.16
144.98
134.80
134.69
134.64
134.38
130.55
130.35
128.20
128.17
128.13
125.66
77.59
77.27
77.02
76.77
43.50
42.36
41.27
36.21
32.09
29.09
28.62
26.87
0.00
Parameter Value
1 Origin Bruker BioSpin GmbH
2 JS-II-104 simon
3 Solvent CDCl3
4 Temperature 294.5
5 Acquisition Date 2013-06-17
6 Spectrometer Frequency 125.79
7 Nucleus 13C
f1 (ppm)

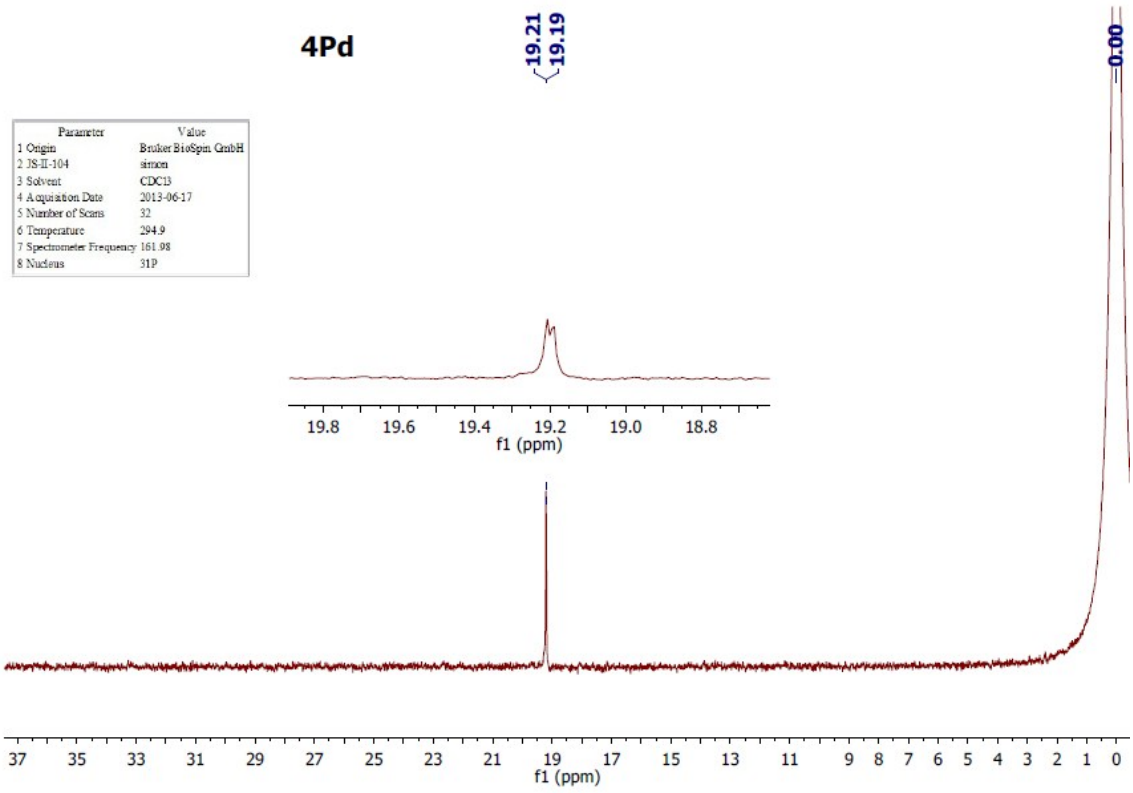
4Pd
19.21
19.19
0.00
Parameter Value
1 Origin Bruker BioSpin GmbH
2 JS-II-104 simon
3 Solvent CDCl3
4 Acquisition Date 2013-06-17
5 Number of Scans 32
6 Temperature 294.9
7 Spectrometer Frequency 161.98
8 Nucleus 31P
f1 (ppm)

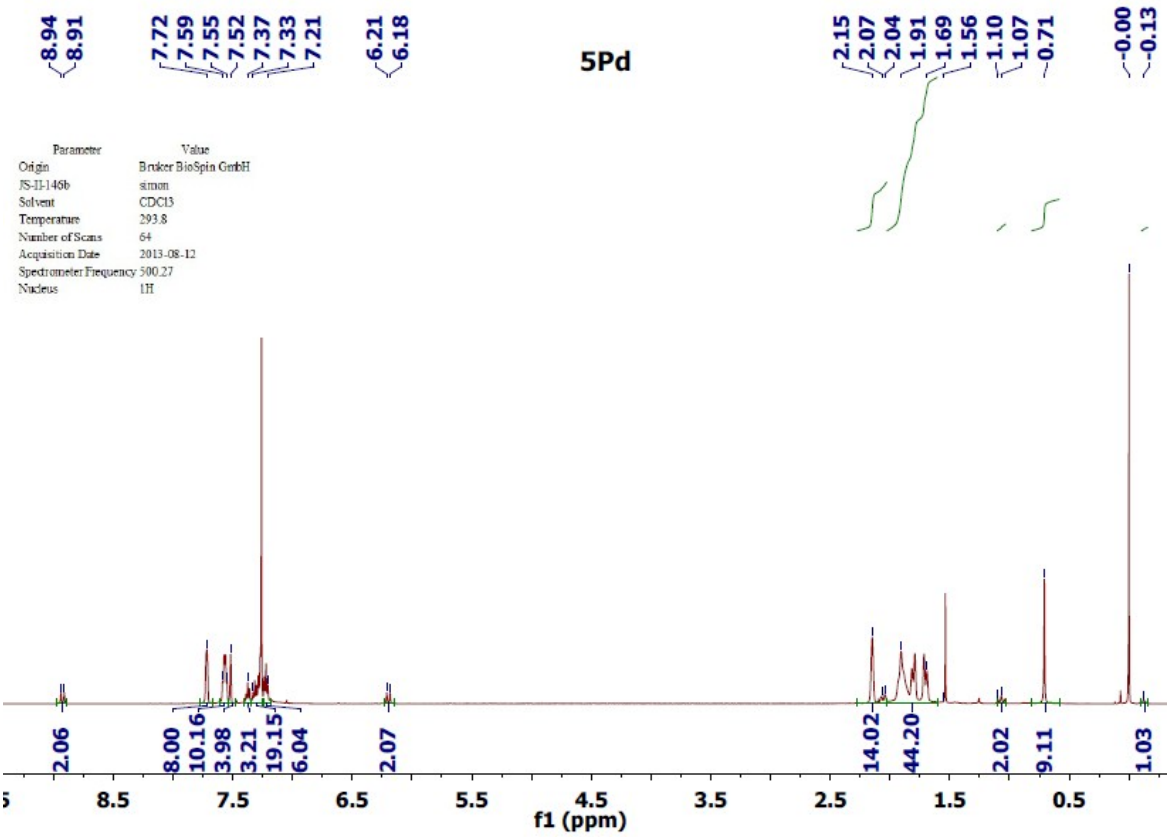
5Pd
8.94
8.91
7.72
7.59
7.55
7.52
7.37
7.33
7.21
6.21
6.18
2.15
2.07
2.04
1.91
1.69
1.56
1.10
1.07
0.71
0.00
0.13
Parameter Value
Origin Bruker BioSpin GmbH
JS-II-146b simon
Solvent CDCl3
Temperature 293.8
Number of Scans 64
Acquisition Date 2013-08-12
Spectrometer Frequency 500.27
Nucleus 1H
2.06
8.00
10.16
3.98
3.21
19.15
6.04
2.07
14.02
44.20
2.02
9.11
1.03
f1 (ppm)

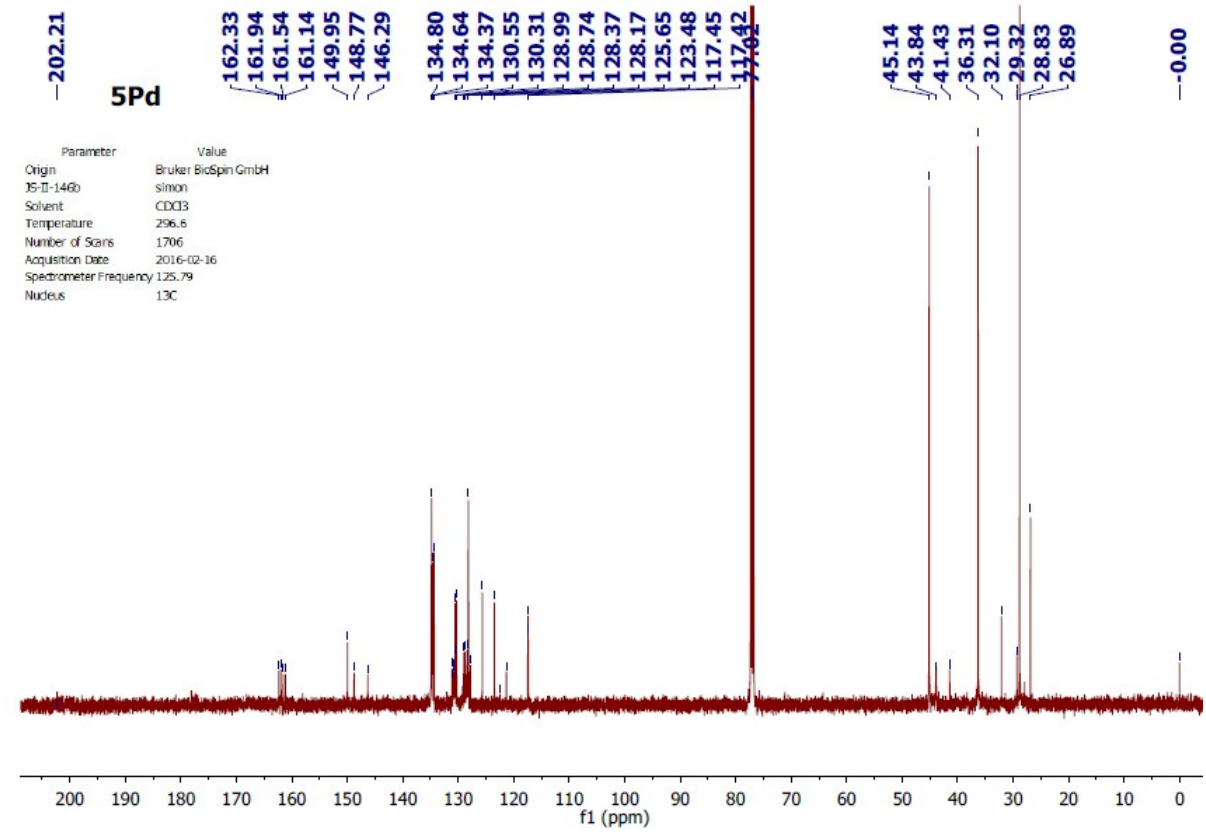
202.21
5Pd
162.33
161.94
161.54
161.14
149.95
148.77
146.29
134.80
134.64
134.37
130.55
130.31
128.99
128.74
128.37
128.17
125.65
123.48
117.45
117.42
77.02
45.14
43.84
41.43
36.31
32.10
29.32
28.83
26.89
0.00
Parameter Value
Origin Bruker BioSpin GmbH
JS-II-146b simon
Solvent CDCl3
Temperature 296.6
Number of Scans 1706
Acquisition Date 2016-02-16
Spectrometer Frequency 125.79
Nucleus 13C
f1 (ppm)

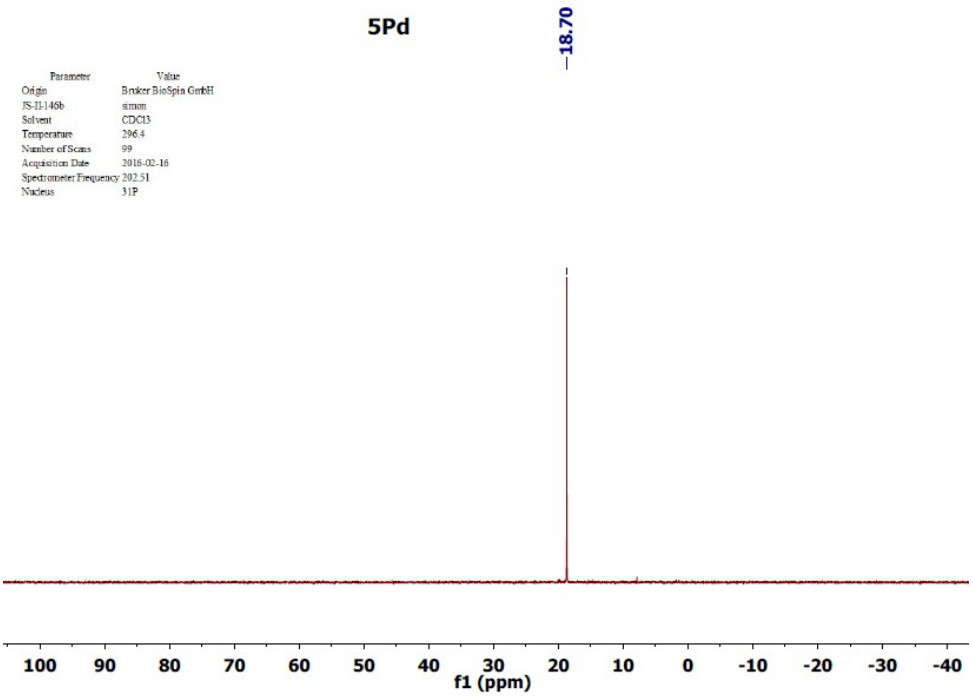
5Pd
18.70
Parameter Value
Origin Bruker BioSpin GmbH
JS-II-146b simm
Solvent CDCl3
Temperature 296.4
Number of Scans 99
Acquisition Date 2016-02-16
Spectrometer Frequency 202.51
Nucleus 31P
100 90 80 70 60 50 40 30 20 10 0 -10 -20 -30 -40
f1 (ppm)

9. References for Supporting Information

1. J. M. Hales, J. Matichak, S. Barlow, S. Ohira, K. Yesudas, J.-L. Brédas, J. W. Perry and S. R. Marder, *Science*, 2010, **327**, 1485.
2. Y. A. Getmanenko, T. G. Allen, H. Kim, J. M. Hales, B. Sandhu, M. S. Fonari, K. Y. Suponitsky, Y. Zhang, V. N. Khrustalev, J. D. Matichak, T. V. Timofeeva, S. Barlow, S.-H. Chi, J. W. Perry and S. R. Marder, *in preparation*.
3. I. Davydenko, S. Barlow, R. Sharma, S. Benis, J. Simon, T. G. Allen, M. W. Cooper, V. Khrustalev, E. V. Jucov, R. Castañeda, C. Ordonez, Z. Li, S.-H. Chi, S.-H. Jang, T. C. Parker, T. V. Timofeeva, J. W. Perry, A. K.-Y. Jen, D. J. Hagan, E. W. Van Stryland and S. R. Marder, *J. Am. Chem. Soc.*, 2016, **138**, 10112.
4. R. Wizinger and H. J. Angliker, *Helv. Chim. Acta*, 1966, **49**, 2046.
5. Y. Nagao, T. Osawa, K. Kozawa and T. Urano, *Shikizai Kyokaishi*, 2005, **78**, 12.
6. S. Barlow, J.-L. Brédas, Y. A. Getmanenko, R. L. Gieseking, J. M. Hales, H. Kim, S. R. Marder, J. W. Perry, C. Risko and Y. Zhang, *Mater. Horiz.*, 2014, **1**, 577.
7. J.-D. Chai and M. Head-Gordon, *Phys. Chem. Chem. Phys.*, 2008, **10**, 6615.
8. J.-D. Chai and M. Head-Gordon, *J. Chem. Phys.*, 2008, **128**, 084106.
9. T. H. Dunning, *J. Chem. Phys.*, 1989, **90**, 1007.
10. D. Feller, *J. Comput. Chem.*, 1996, **17**, 1571.
11. K. L. Schuchardt, B. T. Didier, T. Elsethagen, L. Sun, V. Gurumoorthi, J. Chase, J. Li and T. L. Windus, *J. Chem. Inf. Model.*, 2007, **47**, 1045.
12. H. Nakatsuji and K. Hirao, *J. Chem. Phys.*, 1978, **68**, 2053.
13. N.Nakatsuji, *Chem. Phys. Lett.*, 1978, **59**, 362.
14. M. J. Frisch, G. W. Trucks, H. B. Schlegel, G. E. Scuseria, M. A. Robb, J. R. Cheeseman, G. Scalmani, V. Barone, B. Mennucci, G. A. Petersson, H. Nakatsuji, M. Caricato, X. Li, H. P. Hratchian, A. F. Izmaylov, J. Bloino, G. Zheng, J. L. Sonnenberg, M. Hada, M. Ehara, K. Toyota, R. Fukuda, J. Hasegawa, M. Ishida, T. Nakajima, Y. Honda, O. Kitao, H. Nakai, T. Vreven, J. A. Montgomery, J. E. Peralta, F. Ogliaro, M. Bearpark, J. J. Heyd, E. Brothers, K. N. Kudin, V. N. Staroverov, T. Keith, R. Kobayashi, J. Normand, K. Raghavachari, A. Rendell, J. C. Burant, S. S. Iyengar, J. Tomasi, M. Cossi, N. Rega, J. M. Millam, M. Klene, J. E. Knox, J. B. Cross, V. Bakken, C. Adamo, J. Jaramillo, R. Gomperts, R. E. Stratmann, O. Yazyev, A. J. Austin, R. Cammi, C. Pomelli, J. W. Ochterski, R. L. Martin, K. Morokuma, V. G. Zakrzewski, G. A. Voth, P. Salvador, J. J. Dannenberg, S. Dapprich, A. D. Daniels, O. Farkas, J. B. Foresman, J. V. Ortiz, J. Cioslowski and D. J. Fox, *Gaussian 09 Revision B.01*, Gaussian Inc.: Wallingford CT, 2010.
15. R. L. Gieseking, S. Mukhopadhyay, C. Risko, S. R. Marder and J.-L. Brédas, *Chem. Mater.*, 2014, **26**, 6439.
16. R. L. Gieseking, S. Mukhopadhyay, S. B. Shiring, C. Risko and J.-L. Brédas, *J. Phys. Chem. C*, 2014, **118**, 23575.
17. B. Hess, C. Kutzner, D. van der Spoel and E. Lindahl, *J. Chem. Theory Comput.*, 2008, **4**, 435.
18. W. L. Jorgensen, D. S. Maxwell and J. Tirado-Rives, *J. Am. Chem. Soc.*, 1996, **118**, 11225.
19. S. Das, D. Bwambok, B. El-Zahab, J. Monk, S. L. de Rooy, S. Challa, M. Li, F. R. Hung, G. A. Baker and I. M. Warner, *Langmuir*, 2010, **26**, 12867.
20. M. R. Ferdinandus, M. Reichert, T. R. Ensley, H. Hu, D. A. Fishman, S. Webster, D. J. Hagan and E. W. Van Stryland, *Opt. Mater. Expr.*, 2012, **2**, 1776.
21. M. Sheik-Bahae, A. A. Said, T.-H. Wei, D. J. Hagan and E. W. Van Stryland, *IEEE J. Quantum. Electron.*, 1990, **26**, 760.
22. T. R. Ensley, H. Hu, M. Reichert, M. R. Ferdinandus, D. Peceli, J. M. Hales, J. W. Perry, Z. a. Li, S.-H. Jang, A. K.-Y. Jen, S. R. Marder, D. J. Hagan and E. W. Van Stryland, *J. Opt. Sci. Am. B*, 2016, **33**, 780 (Erratum: *J. Opt. Sci. Am. B*, 2016, **33**, 1007).